JOC The Journal of Organic Chemistry

Article

Guidelines for #-Lactam Synthesis: Glycal Protecting Groups Dictate Stereoelectronics and [2+2] Cycloaddition Kinetics

Anant S. Balijepalli, James H. McNeely, Aladin Hamoud, and Mark W. Grinstaff

J. Org. Chem., **Just Accepted Manuscript** • DOI: 10.1021/acs.joc.0c00510 • Publication Date (Web): 26 Aug 2020

Just Accepted

is published by the American Chemical Society. 1155 Sixteenth Street N.W., Washington, DC 20036

Guidelines for β-Lactam Synthesis: Glycal Protecting Groups Dictate Stereoelectronics and [2+2] Cycloaddition Kinetics

Anant S. Balijepalli[1,†] James H. McNeely[2,†], Aladin Hamoud[2], and Mark W. Grinstaff[1,2,*]

1.) Department of Biomedical Engineering, Boston University, Boston, MA, 02215

2.) Department of Chemistry, Boston University, Boston, MA, 02215

KEYWORDS: Glycals, Cycloaddition, Protecting Groups, Stereoelectronics, β-Lactams, Density Functional Theory (DFT) Calculations

ABSTRACT: The alkene-isocyanate cycloaddition method affords β-lactams from glycals with high regio- and stereoselectivity, but the factors that determine substrate reactivity are poorly understood. Thus, we synthesized a library of 17 electron-rich alkenes (glycals) with varied protecting groups to systematically elucidate the factors that influence their reactivity towards the electron-poor trichloroacetyl isocyanate. The experimentally determined reaction rates exponentially correlate with the computationally-determined HOMO-LUMO gap and NBO (natural bond orbital) valence energies. The electron withdrawing ability of the protecting groups, but not bulk, impacts the electron density of the glycal allyloxocarbenium system when oriented *pseudo*-axially (i.e., stereoelectronics). In this conformation, ring $\sigma_{C\text{-}O}$* orbitals oriented anti-periplanar to the allyloxocarbenium system decrease glycal reactivity via negative hyperconjugation as protecting group electron withdrawal increases. Transition state calculations reveal that protecting group stereoelectronics direct the reaction to proceed via an asynchronous one-step mechanism through a zwitterionic species. The combined experimental and computational findings, along with experimental validation on an unknown glycal, provide insight on the reaction mechanism and the role of distant protecting groups in glycal reactivity. Together, these studies will aid in the synthesis of new β-lactam antibiotics, β-lactamase inhibitors, and bicyclic carbohydrate-β-lactam monomers prepared by the alkene-isocyanate method.

INTRODUCTION

Lactams are an important class of functional group integral to several key medicinal and material advances in the 20th century.[1–5] The discovery of penicillin, whose β-lactam ring is essential for its inhibitory action against bacterial cell wall synthesis, in 1928 led to the facile treatment of a wide array of common bacterial ailments with a resulting significant increase in life expectancy.[1–3] β-lactam containing compounds are aliphatic ring systems containing an amide bond. Many β-lactam compounds are bicyclic structures whose properties depend upon heteroatom substitution (Chart 1).[3,6–8]

For example, β-lactams fused to a sulfur-substituted five-membered ring (i.e., penicillin derivatives) exhibit significantly divergent antibiotic properties than when fused to an unsaturated oxygen-substituted six-membered ring (i.e., oxacephem derivatives): the aminopenicillin amoxicillin is more efficacious against *S. aureus* than *P. aeruginosa* while the converse is observed for the slightly modified carboxypenicillin carbenicillin.[9,10] Current strategies to circumvent antibiotic resistance include synthesizing β-lactam antibiotics with different ring sizes and heteroatom substitution[1–4,11,12] as well as preparing β-lactamase inhibitors such as the oxabicyclic clavulanic acid.[4,13–15] This avenue of research remains a high priority in light of the inevitable obsolescence of traditional antibiotics such as penicillin and amoxicillin.

In addition to the medicinal importance of the β-lactam structure, the synthesis of Nylon 6 in 1938 via caprolactam (Chart 1D) documented its importance as a key structural motif in monomers for ring-opening polymerization. Nylon-based polymers are used widely in consumer products such as clothing, carpets, and automobile parts.[16] Today, more structurally complex β-lactam monomers are being synthesized including those resembling naturally-occurring polypeptides[17–19] and such nylon 3 polymers (Chart 1E) are effective antimicrobial[19–23] and gene delivery[24] agents. We recently described a new class of carbohydrate polymers, prepared from the anionic ring opening polymerization of a bicyclic sugar-β-lactam monomer[25,26] (Chart 1F), for use as cyropreservants[27], antimicrobial agents[28], and as lectin agonists.[29]

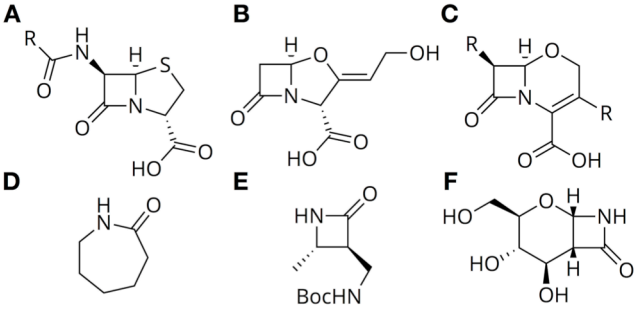

Chart 1. Common β-lactam antibiotics, β-lactamase inhibitors, and lactam monomers. (A): penicillin family; (B): clavulanic acid; (C): oxacephem ring structure; (D): caprolactam; (E): nylon-3 monomer; (F): polyamidosaccharide monomer.

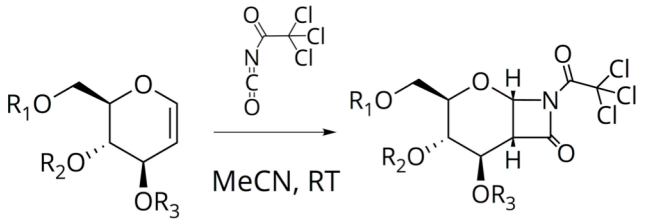

Scheme 1. Cycloaddition reaction of fully-protected glycal and trichloroacetyl isocyanate (TCAI) yields bicyclic β-lactams with high stereoselectivity.

β-lactams are commonly synthesized via the Staudinger synthesis due to its versatility and relative accessibility.[30–33] Depending on the steric and electronic properties of the substituents on either the ketene or the imine, the reaction may vary in geometry of the initial attack by the imine and in the subsequent isomerization of the zwitterionic intermediate.[32,33] As a result, products are usually obtained as a *cis*/*trans* racemic mixture that, despite the readily available imine and ketene precursors, presents a significant hurdle to the synthesis of new enantiopure β-lactams.[30–33] In addition to poor stereochemical control, the ketene substrate is unstable in many cases[34,35] and must be generated *in situ* from an acyl chloride and tertiary amine or from the Wolff rearrangement of α-diazocarbonyl compounds.[36] Alternative methods to synthesize β-lactams include the expansion of aziridine rings[37,38] and the Kinugasa reaction[39,40], but the starting materials for these methods are not widely available commercially.

In contrast, the reaction of electron-deficient isocyanates with electron-rich alkenes is a robust and relatively mild method to synthesize β-lactams.[39,41] Unlike the Staudinger synthesis, this reaction offers less flexibility in the functionality of the starting reagents, with the majority of examples utilizing activated isocyanates such as chlorosulfonyl isocyanate (CSI), *p*-tolunesulfonyl isocyanate, trifluoroacetyl isocyanate, and trichloroacetyl isocyanate (TCAI).[39–43] Of note, while the Staudinger synthesis is generally accepted to follow a stepwise mechanism, findings from computational studies on small model compounds (e.g., ethylene and isocyanic acid) have led to proposals of both stepwise and concerted mechanisms between sufficiently electron-rich alkenes and electron-deficient isocyanates.[44–47] Herein, we present a systematic study to elucidate the influence of protecting group stereoelectronics and solvents on the reaction kinetics of eighteen glycals with combinations of common hydroxyl protecting groups (Table 1) and TCAI (Scheme 1). The goals of this multifaceted study are to: 1) identify the protecting groups that are stable to cycloaddition with TCAI; 2) measure the kinetics of the cycloaddition reaction between protected glycals and TCAI; and, 3) use conformer-weighted Kohn-Sham and natural bond orbital calculations to support our experimental observations and propose a model that identifies negative hyperconjugation as an important factor in glycal allyloxocarbenium reactivity. We hypothesize that glycals with protecting groups adopting a *pseudo*-axial ($^5H_4$) orientation possess a favorable periplanar orientation of ring $\sigma_{C\text{-}O}$*, with respect to the allyloxocarbenium system, thus facilitating negative hyperconjugation and modulation of its reactivity.

Table 1. List of selected protected glycal substrates.

Substrate	Synthetic scheme	R_1	R_2	R_3
1	-	Ac	Ac	Ac
2	-	Bn	Bn	Bn
3	-	Me	Me	Me
4	A	Et	Et	Et
5	A	TES	TES	TES
6	A	PMB	PMB	PMB
7	A	Troc	Troc	Troc
8	A	MOM	MOM	MOM
9	B1	Bn	Bn	Bn
10	B2	TIPS	Ac	Ac
11	B2	TIPS	PMB	PMB
12	B2	TIPS	Bn	Bn
13	B2	Ac	Bn	Bn
14	B2	Me	Bn	Bn
15	B2	Troc	Bn	Bn
16	B2	Tr	Bn	Bn
17	B2	DMT	Bn	Bn

RESULTS AND DISCUSSION

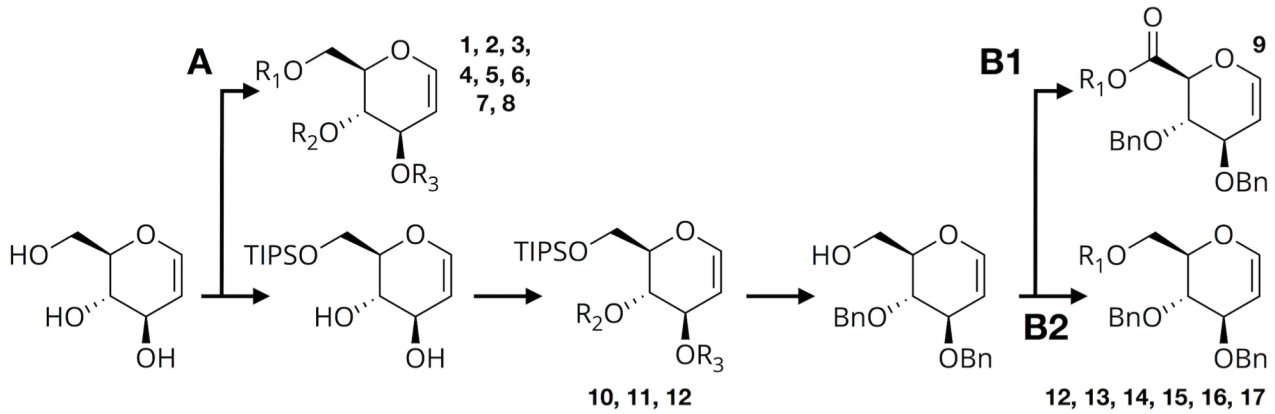

Scheme 2. Synthetic design for regioselectively and orthogonally protected glycals. Scheme A: protection of all 3 hydroxyl functionalities with the same protecting group. Scheme B: regioselective protection by TIPS group followed by selective protection of the 3'- and 4'-OH; the silyl group was removed and the 6'-OH either (1) oxidized and protected or (2) orthogonally protected.

Chmielewksi and Kaluza studied the reactions of both CSI and TCAI with protected glycals in order to yield oxabicyclic β-lactam antibiotic structures including clavams and oxacephems.[41,48–52] The authors pose several empirical observations including that cycloadducts between glycals and CSI were susceptible to degradation at higher temperatures, nonpolar protecting groups afforded higher yields, side products were formed due to a competing [4+2] cycloaddition reaction, rearrangement of the transition state to a stable α, β-unsaturated amide, and a high stereoselectivity towards *trans*-substituted β-lactams with respect to the C-3 position.[48,49]. In agreement with the observations noted by Chmielewksi, we obtain enantiopure bicyclic β-lactam structures in higher yield using tri-*O*-*tert*-butyldimethylsilyl (TBDMS) protected glycals as opposed to tri-*O*-benzyl protected glycals.[25] When extending this methodology to glycals with combinations of protecting groups, however, we observed highly variable reaction outcomes. Consequently, we undertook a comprehensive and systematic experimental and computational study to: 1) determine the scope of reaction in terms of glycal composition; 2) understand the advantages and limitations of the reaction; 3) propose a mechanism; and, 4) develop a set of guidelines to inform the future synthesis of β-lactams.

The most commonly used protecting groups for the hydroxyl functionality span a wide range of steric bulk and electron withdrawing ability that are likely to influence the outcome of the cycloaddition reaction (Schemes 1 and 2, Table 1). For example, *O*-trityl protecting groups are highly electron rich and bulky enough to selectively protect the primary 6' OH functionality while *O*-acetyl protecting groups are comparatively small and possess some electron withdrawing character, due to the neighboring carbonyl. As shown in Scheme 2 and Table 1, the 17 substrates include glycals protected by the same protecting group at all 3 positions, glycals that are regioselectively protected at the 6' OH, and a glycal with a carboxylate at the 6' carbon. While substrates such as **8,** the tri-*O*-methoxymethyl (MOM) protected glycals, possess less steric bulk and less electron withdrawing capacity, substrates such as **7**, the tri-*O*-2,2,2-trichloroethyl carbonate (Troc) protected glycals, are bulky and highly electron withdrawing.

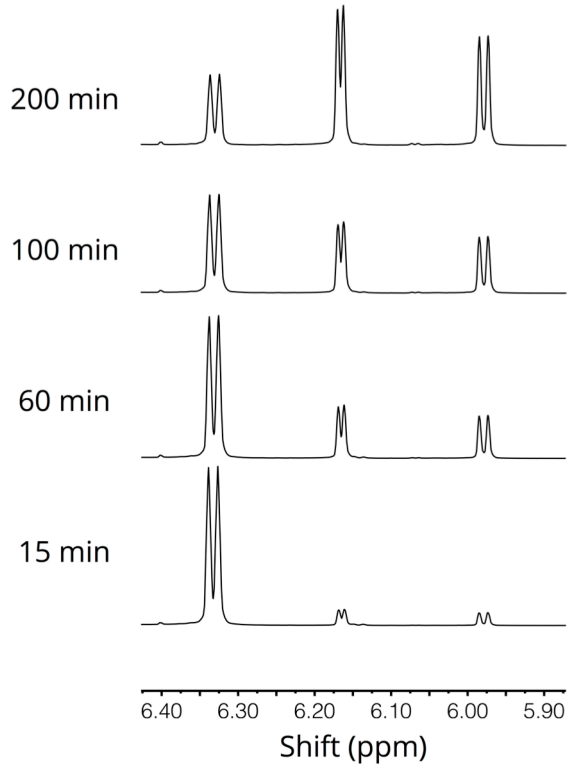

Figure 1. Example ^{1}H-NMR data during cycloaddition reaction at 15, 60, 100, and 200 minutes for 3,4,6-tri-*O*-ethyl-D-glucal. The H1 peak corresponding to the starting material diminishes in intensity over time at δ ≈ 6.33 ppm while the H1 peaks corresponding to the [2+2] product (δ ≈ 5.98 ppm) and [4+2] product (δ ≈ 6.17 ppm) gradually increase in intensity over time.

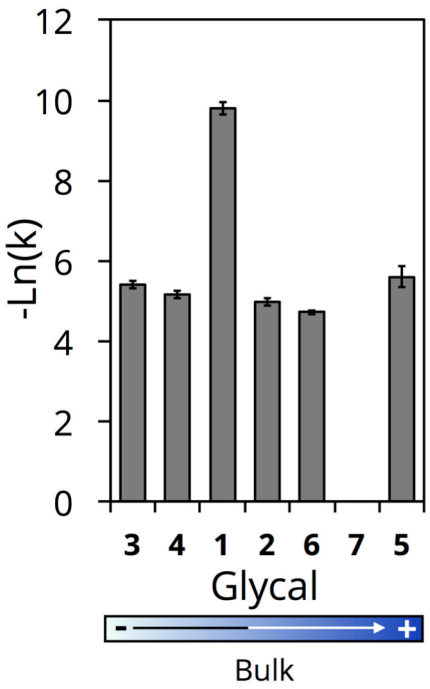

Figure 2. Relationship between reaction rate and steric bulk (qualitatively ordered from lowest to highest). **3** – Tri-*O*-methyl, **4** – Tri-*O*-ethyl, **1** – Tri-*O*-acetyl, **2** – Tri-*O*-benzyl, **6** – Tri-*O*-PMB, **7** – Tri-*O*-Troc (no reaction), **5** – Tri-*O*-TES.

In order to synthesize the library of regioselectively modified glycals (**10**-**18**), as shown in Scheme 2, we reacted the commercially available D-glucal with the bulky triisopropylsilyl chloride (TIPSCl) to selectively protect the 6' OH position followed by acetylation, *p*-methoxybenzylation, or benzylation of the remaining positions to yield substrates **10**-**12**, respectively (yields 71-79%; see SI). After tetrabutylammonium fluoride (TBAF) mediated desilylation, the 6' OH position (yield 89%) was either further protected orthogonally or oxidized by TEMPO and benzyl protected (yields varied from 32 to 84%). Following purification, we dissolved the substrate in 300 μL of CD_3CN (0.5 M) and added 2.0 eq of TCAI prior to beginning the NMR study. Surprisingly, we were unable to detect product formation for the protected oxidized glycal (Substrate **9**) as well as the tri-*O*-Troc glycal (Substrate **7**) over 4 days of monitoring. In addition, the tri-*O*-MOM glycal (**8**), 6-*O*-trityl glycal (**16**), and 6-*O*-dimethoxytrityl (DMT) glycal (**17**) were unstable to the reaction conditions as several peaks in the ^{1}H-NMR spectra were consistent with species from a degradation reaction. In all cases, the relative composition of starting materials and products in the reaction mixture were readily determined by NMR due to clear separation between the respective peaks in the ^{1}H-NMR spectra (Figure 1).

We identified the C1 protons of the starting material as well as those of the [2+2] and [4+2] products by $^{1}H^{13}C$-HSQC (Figure S1) and calculated the ratio of the integration of the C1 proton of the starting material to the total integration of all components to determine the percent of starting material remaining in the mixture. Although other side products, and in certain cases stereoisomers, were present in some reactions, these were formed in negligible quantities (< 5% of total composition at reaction completion). The consumption of starting material in all reactions in acetonitrile followed first-order kinetics (Figure S2) from which we extracted the reaction rate as the decay constant.

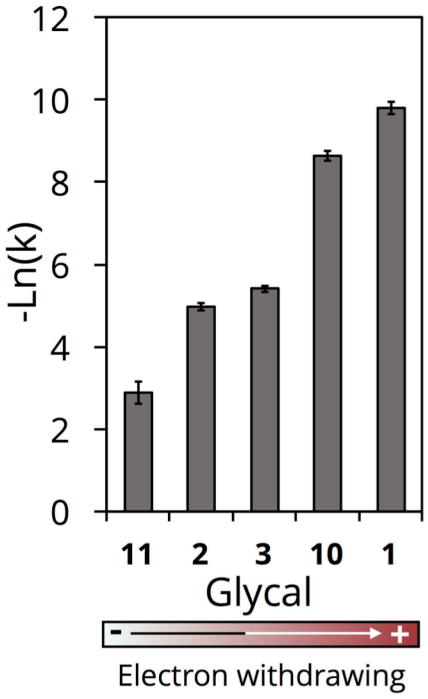

Figure 3. Comparison of experimentally observed reaction rates of glycals with protecting groups ordered from least electron withdrawing to most electron withdrawing. 11: 3,4-di-O-PMB-6-TIPS-D-glucal; 2: 3,4,6-tri-O-benzyl-D-glucal; 3: 3,4,6-tri-O-methyl-D-glucal; 10: 3,4-di-O-acetyl-6-O-TIPS-D-glucal; 1: 3,4,6-tri-O-acetyl-D-glucal.

Previous work in our group, in agreement with Chmielewksi's observations, indicated that bulky non-polar protecting groups increase the reaction rate and [2+2] product yield.[25] To test this hypothesis, we experimentally determined reaction rates of substrates **1-6,** which each possess three identical protecting groups. The protecting group bulk was qualitatively ranked (e.g., acetyl < triethylsilyl) and compared to these experimental rates and, as shown in Figure 2 (and Table 2), no clear relationship is observed. For example, reactions with glycals possessing large triethylsilyl groups proceed with nearly identical rate (0.0037 s^{-1}) to glycals with methyl protecting groups (0.0045 s^{-1}). Moreover, glycals with the bulky Troc protecting group did not react with TCAI unlike tri-*O*-acetyl (less bulky) protected glycals that react with a rate of 0.000055 s^{-1}.

Given the poor relationship between protecting group bulk and reaction rate, we reason that the rate acceleration observed for certain bulky protecting groups is a consequence of their reduced electron withdrawing ability. Electron withdrawing substituents are known to significantly influence the stereochemistry of Staudinger reaction products due to their effect on the reaction rates during the step-wise mechanism.[32,33] Additionally, Jiao et. al reported that the Hammett constants of the substituents on the imine and ketene in the Staudinger synthesis predicted the *cis*/*trans* ratio.[32] In order to empirically test this hypothesis, we ranked five substrates with protecting groups from the least to most electron withdrawing based on the experimentally determined reaction rates in acetonitrile. As shown in Figure 3, the reaction rate reduces by ~1000 fold from ~0.05 s^{-1} for the less electron withdrawing 3,4-di-*O*-*p*-methoxybenzyl-6-*O*-triisopropylsilyl protected (**11**) to ~0.00005 s^{-1} for the more electron withdrawing tri-*O*-acetyl protected glycal (**1**). These data show that the protecting groups at each position on the glycal, including the distant 6'OH influence the electronics of the alkene. Indeed, the sim-

Table 2. Calculated HOMO energies for selected protected glycal substrates in both gas phase and acetonitrile solvent model (n.r. = no reaction observed over 4 days).

Substrate	Glycal (-D-glucal)	ε_{HOMO} (gas phase) (eV)	ε_{HOMO} (solvent) (eV)	ε_{LUMO}-ε_{HOMO} (gas phase) (eV)	ε_{LUMO}-ε_{HOMO} (solvent) (eV)	Reaction rate (s^{-1})
1	**tri-*O*-acetyl**	**-6.959**	**-6.829**	**4.741**	**4.743**	**0.000055**
2	**tri-*O*-benzyl**	**-6.581**	**-6.584**	**4.363**	**4.498**	**0.0069**
3	**tri-*O*-methyl**	**-6.461**	**-6.515**	**4.243**	**4.429**	**0.0045**
4	**tri-*O*-ethyl**	**-6.335**	**-6.378**	**4.117**	**4.292**	**0.0057**
5	**tri-*O*-TES**	**-6.354**	**-6.439**	**4.136**	**4.353**	**0.0037**
6	**tri-*O*-PMB**	**-6.443**	**-6.551**	**4.225**	**4.465**	**0.0088**
7	**tri-*O*-Troc**	**-7.330**	**-7.074**	**5.112**	**4.988**	**n.r.**
9	**Benzyl di-*O*-benzyl-D-glucuronal**	**-6.587**	**-6.706**	**4.369**	**4.620**	**n.r.**
10	**3,4-di-*O*-acetyl-6-*O*-TIPS**	**-6.774**	**-6.717**	**4.556**	**4.631**	**0.00018**
11	**3,4-di-*O*-PMB-6-*O*-TIPS**	**-6.232**	**-6.549**	**4.014**	**4.463**	**0.056**
12	**3,4-di-*O*-benzyl-6-*O*-TIPS**	**-6.464**	**-6.478**	**4.246**	**4.392**	**0.031**
13	**3,4-di-*O*-benzyl-6-*O*-acetyl**	**-6.486**	**-6.599**	**4.268**	**4.513**	**0.0011**
14	**3,4-di-*O*-benzyl-6-*O*-methyl**	**-6.384**	**-6.527**	**4.166**	**4.441**	**0.0031**
15	**3,4-di-*O*-benzyl-6-*O*-Troc**	**-6.784**	**-6.714**	**4.566**	**4.628**	**0.00036**

ple modification of the 6' OH to a TIPS protecting group increases the reaction rate nearly 10-fold compared to the peracetylated glycal (**10** vs **1**). In addition, strongly electron withdrawing components at positions far from the alkene (e.g., 6-*O*-Troc) significantly diminish its reactivity even with benzyl protecting groups at 3' and 4' OH (**15** vs **2;** Table 2).

The reaction rate trends highlighted here resemble those observed for glycosylation reactions, where protecting group choices lead to empirically determined "armed", "disarmed", and "superarmed" substrates.[53–60] Like these glycosylation reactions, the electron density of the ring oxygen plays a major role in tuning reactivity; the allyloxocarbenium system is modulated through participation in negative hyperconjugation with neighboring periplanar σ* orbitals. In both cases, less electron withdrawing protecting groups, such as benzyl protecting groups, destabilize the neighboring ring σ* orbital and thereby prevent negative hyperconjugation from the allyloxocarbenium system.

To further investigate how protecting groups modulate glycal electronics as well as understand the disparities in reaction rates, we performed DFT calculations (PBE0/DEF2-TZVP/D3BJ[/SMD(ACN)]) on the minimum energy structure with $^5H_4$ conformation (*vide infra*) of all 14 substrates (Figure S3-S16). We extracted the highest occupied molecular orbital energy (in some cases, the HOMO did not correspond to the alkene; in this situation the π bond energy was extracted) in eV. These calculations were also performed with an acetonitrile implicit solvation model. Table 2 lists the calculated HOMO values in both gas phase and solvent. Importantly, protecting groups at relatively distant positions from the alkene influence the HOMO energy and support our qualitative ordering of the electron withdrawing ability as well as hyperconjugation between the ring oxygen and neighboring σ* orbitals. For example, when comparing substrate **15** and substrate **12** with identical 3'- and 4'-OH benzyl protection, a small change at the 6'-OH position from *O*-Troc protection to *O*-TIPS protection affords a significant increase in HOMO energy (372 meV; ~33% of the entire range of HOMO for all substrates).

We note here that these HOMO energies are directly proportional to the nucleophilicity indices described by Domingo[61], and as such the correlation we obtain in the framework of FMO theory is expected to be similarly obtained based on theoretical description in the framework of conceptual DFT. Work is currently being performed to explore the reaction pathways of these glycals in the context of molecular electron density theory[62].

A quantitative relationship between HOMO energies and experimentally observed reaction rates exist that supports our hypothesis that protecting groups influence alkene reactivity via modulating negative hyperconjugation. As shown in Figure 4A, a logarithmic plot of the observed reaction rates vs. the gas phase HOMO-LUMO gap calculations affords a linear relationship (R^2=0.75). When the implicit solvation model HOMO-LUMO gap calculations are used (Figure 4B), this linear relationship diminishes slightly (R^2=0.61). Importantly, reaction rates increase logarithmically with decreasing HOMO-LUMO gaps, strongly resembling an Arrhenius relationship between reaction rate and activation energy. While previous reports have established an Arrhenius relationship for the [2+2] cycloaddition between CSI and fluorinated alkenes with respect to temperature changes[63], we demonstrate this same relationship with TCAI by varying the substrate energetic profile and holding temperature constant. Of the substrates investigated, the tri-*O*-Troc protected glycal (**7**) and benzyl-protected oxidized glycal (**9**) did not react with TCAI over 5 days of reaction monitoring. The low HOMO energy (-7.330 eV) of **7** is consistent with this observation. Interestingly, **9** did not react with the isocyanate despite having a HOMO energy ~370 meV greater than that of **1,** the tri-*O*-acetyl protected glycal. In addition, the sterically hindered tri-*O*-TES protected glycal (**5**, green) deviated significantly from the linear model, with a reaction rate significantly slower than expected given its high calculated HOMO value of -6.354 eV (discussed further *vide infra*).

Although a linear relationship between HOMO-LUMO gap and reaction rate is observed, we identified several modeling limitations to address in order to improve our analyses. For example, the modeled HOMO for certain protected glycals such as tri-*O*-PMB and 3,4-di-*O*-PMB-6-*O*-TIPS (substrates **6** and **11**) are delocalized (Figure S8, S12), with significant contributions from the aryl protecting groups. Additionally, the flexibility of side chains for each substrate gives rise to a large number of conformers at each hydroxyl position. These conformers, many of which lie within 2 kcal/mol of the global minimum energy structure, include protecting groups oriented either *pseudo*-axially ($^5H_4$) or *pseudo*-equatorially ($^4H_5$) to the glycal ring. The orientation of these protecting groups affects the orientation of the ring $\sigma_{C\text{-}O}$* orbitals, and as a result, impacts the alkene's electronics. Protecting group orientation plays a significant role in glycosylation reactions, and, for example, rationalizes the deactivating effect of the 4,6-*O*-benzylidene protecting group.[58,60] Bols[64] and Crich[65], among others propose that the fused ring system introduces a torsion-

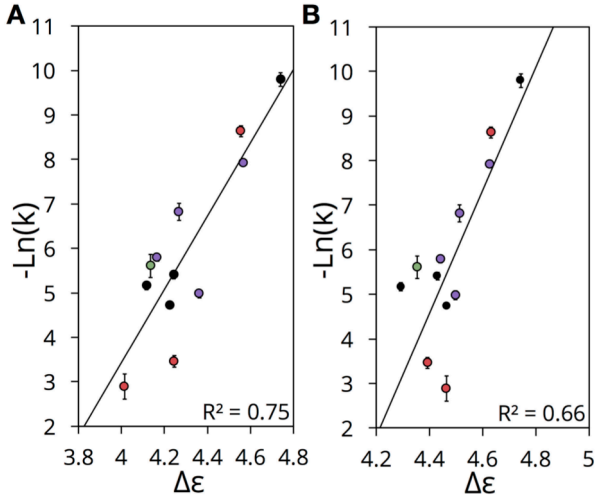

Figure 4. (A) Linear correlation between the logarithm of cycloaddition reaction rate and the corresponding HOMO-LUMO gap between glycal and trichloroacetyl isocyanate (LUMO calculated to be -2.2178 eV) in gas phase. (B) Linear correlation between the logarithm of cycloaddition reaction rate and the corresponding HOMO-LUMO gap between glycal and trichloroacetyl isocyanate (LUMO calculated to be -2.0858 eV) in an acetonitrile implicit solvation model. The residual of the lone outlier (tri-*O*-TES protected glycal) was found to exceed 3 standard deviations of the mean of residuals, supporting its exclusion from the linear regression. Red circles – series of 6-*O*-TIPS protected glycals; purple circles – series of 3,4-di-*O*-benzyl protected 6-*O* regioselectively protected glycals; green circle – tri-*O*-TES protected glycal.

Table 3. Experimentally determined vicinal coupling constants between H4 and H5 as determined by ^{1}H-NMR. (n.d. = not determined)

Substrate	Glycal	$^3J_{H4H5}$ (Hz)
1	**tri-*O*-acetyl**	**7.3**
2	**tri-*O*-benzyl**	**8.2**
3	**tri-*O*-methyl**	**8.3**
4	**tri-*O*-ethyl**	**8.5**
5	**tri-*O*-TES**	**n.d.**
6	**tri-*O*-PMB**	**8.4**
7	**tri-*O*-Troc**	**8.4**
9	**benzyl di-*O*-benzyl-D-glucuronal**	**3.1**
10	**3,4-di-*O*-acetyl-6-*O*-TIPS**	**n.d.**
11	**3,4-di-*O*-PMB-6-*O*-TIPS**	**n.d.**
12	**3,4-di-*O*-benzyl-6-*O*-TIPS**	**n.d.**
13	**3,4-di-*O*-benzyl-6-*O*-acetyl**	**8.3**
14	**3,4-di-*O*-benzyl-6-*O*-methyl**	**8.3**
15	**3,4-di-*O*-benzyl-6-*O*-troc**	**8.4**

al restriction, locking the glycal in the $^4H_5$ orientation and disfavoring the formation of a flattened oxacarbenium ion.

To further probe these stereoelectronic factors, we identified all conformers for a given glycal within ~30 eV from the minimum energy structure at the PBE0/DEF2-TZVP/D3BJ/CPCM(ACN)//PBE0/D3BJ/DEF2-SVP//MMFF94 level. While the entire conformational window for substrates such as tri-*O*-methyl (substrate **3**) is comprised of only 16 conformers, others with many degrees of freedom, such as 3,4-di-*O*-benzyl-6-*O*-Troc (substrate **15**) were limited to ~100 conformers to make the calculations affordable. Glycals with $^4H_5$ orientation comprise a significant proportion of the selected conformers (not expected to contribute to reaction kinetics, *vide infra*) in all cases except for the tri-*O*-TES protected glycal (substrate **5**), oxidized benzyl protected glycal (substrate **9**), and silyl-protected 6' OH glycals (Table 2). To confirm these computational observations, we measured the $^3J_{H4H5}$ coupling constants to determine their relative orientation. According to the Karplus equation, the vicinal coupling constant decreases to a minimum as the torsion angle between protons passes through 90°; $^3J_{H4H5}$ is accordingly larger for glycals adopting a $^4H_5$ versus a $^5H_4$ orientation. As shown in Table 3, the $^3J_{H4H5}$ for all substrates with measurable coupling constants except **9** are of similar magnitude near 8 Hz, indicating a mixture between $^4H_5$ ($^3J_{H4H5}$ = 11.8 Hz) and $^5H_4$ ($^3J_{H4H5}$ = 2.0 Hz). Given the low (0.6 kcal/mol) theoretical barrier between these two conformations for **1**, these states are expected to rapidly equilibrate in solution.[66] Spectral overlap with H4 and H5 prevented the measurement of $^3J_{H4H5}$ for substrates **5**, **10**, **11**, and **12** despite attempts to separate peaks using solvents such as $(CD_3)_2CO$ and CD_3OH. The predominance of $^5H_4$ within the conformational windows determined computationally for **5** and **9** is supported experimentally in the case of **9**, with a $^3J_{H4H5}$ of only 3.1 Hz. In addition, our group previously found $^3J_{H4H5}$ for a bulky persilylated glycal similar to **5** (tri-*O*-TBDMS-D-glucal) to be 2.8 Hz[25], which is in agreement with the coupling constant found for **9**. Pederson and Bols similarly reported a predominance of the *pseudo*-axial $^5H_4$ orientation with bulky silyl protecting groups, unlike traditional benzylic ether or ester groups, leading to "superarmed" glycosyl donors.[58]

To examine how protecting groups influence stereoelectronics to affect the mechanism of the cycloaddition reaction, we performed transition state calculations on the single minimum energy $^4H_5$ and $^5H_4$ conformers of a subset of the glycals (**1**, **3**, **4**, **12**, and **15**). A summary of the energetic landscape is found in Table 4 and Table SCX1 (see ESI). For each of the $^5H_4$ conformers, the reaction is one-step, yet exhibits significant asynchronicity, with the C-C bond forming prior to ring closure with the C-N bond formation (see Figure 5 and Figure S20). Our calculations additionally indicate that $^4H_5$ and $^5H_4$ conformers, present in all glycals at varying ratios, undergo differing reaction pathways.

The transition state calculations on the $^4H_5$ conformers for **1**, **3**, **4**, **12**, and **15** are summarized in the ESI. The calculated activation barriers suggest that the cycloadditions involving the $^4H_5$ conformers proceed much faster than the corresponding $^5H_4$ conformers. This gave us pause because it is inconsistent with the observed experimental stereoselectivity and the orbital interactions predicted to drive the observed correlation between kinetics and protecting group electron-withdrawing ability.

Upon inspection of the transition state structures and reaction pathways for the $^5H_4$ and $^4H_5$ conformers, however, an explanation presents itself. First, the transition state geometries for the $^4H_5$ conformers are at odds with the $^5H_4$ geometries. Particularly, while the $^5H_4$ structures are expected for an asynchronous one-step [2+2] cycloaddition, the $^4H_5$ geometries are characterized by C_1-C_2-C-N dihedral angles of ~80° (Figure S18). The near-orthogonal orientation of the π-π* partners is unexpected for a concerted cycloaddition, and immediately suggests a two-stage one-step mechanism via a highly asynchronous TS or a two-step mechanism.

Indeed, after following the intrinsic reaction pathway starting from the $^4H_5$ transition state for **3**, we observe that the product did not form after > 7000 steps (Figure 5). While we were unable to locate the second transition state connecting the intermediate with the product, our data indicate that it is characterized by a very low enthalpic barrier (see ESI). Furthermore, the reaction path curvatures following the formation of the C-C bond for the $^4H_5$ conformers were very small. Inspection of the normal modes (Figure S18) show that the second vibrational mode (17 cm^{-1}) is best described as a rotation around the forming C-C bond that moves the TCAI nitrogen

Table 4. Calculated transition state thermodynamic quantities for minimum energy $^5H_4$ conformer of selected substrates

Substrate	$\Delta E^{\ddagger}$	$\Delta H^{\ddagger}$	$\Delta S^{\ddagger}$	$\Delta G^{\ddagger}$	ε_{HOMO} (eV)	ε_{NBO} (kcal/mol)
15	**12.3**	**13.4**	**-13.8**	**27.2**	**-6.714**	**-8.539**
12	**10.6**	**10.4**	**-17.0**	**27.4**	**-6.478**	**-8.424**
4	**9.6**	**10.1**	**-15.4**	**25.5**	**-6.378**	**-8.396**
3	**10.9**	**11.4**	**-14.9**	**26.3**	**-6.515**	**-8.391**
1	**12.5**	**12.8**	**-15.3**	**28.2**	**-6.829**	**-8.667**

away from the C_1 carbon, out-of-phase with the motion governed by the imaginary mode. Each of these observations suggests that canonical transition state theory is not suitable to describe the reaction pathways for the $^4H_5$ conformers.

Singleton's group studied the pathways of the reaction between ketenes with cyclopentadiene and cis-2-butene[67,68]. They note the following interesting observations that are directly relevant to the work described in this manuscript: 1) the geometry of the transition state calculated for the cycloaddition of cis-2-butene with dichloroketene shares similar characteristics with the $^4H_5$ transition state structures calculated in this work with an orthogonal approach of the two interacting fragments at the CCSD(T)/6-311++G**/PCM(CH_2Cl_2) level of theory; 2) An entropic barrier for the formation of the second C-C bond in the cycloaddition of dichloroketene with cis-2-butene was proposed for which there was no enthalpic barrier, but was termed an 'entropic transition state'. This entropic transition state was found to be rate-limiting based on direct dynamics trajectories.

Spurred on by the success of Singleton's group, we undertook a detailed study of the dynamics of the reaction pathways for the $^4H_5$ and $^5H_4$ conformers. While a full account of the results will be given in a future publication, the preliminary results support our previous assumption that only the $^5H_4$ participate in the [2+2] formation of β-lactams in these glycal-TCAI systems. Of 100 sampled trajectories starting from the transition state for the $^4H_5$ conformer of **3**, not a single one resulted in the formation of the desired product, and greater than 95% re-crossed to form the reactants (Figure S22). This can be compared with a 23% product formation for the trajectories started from the $^5H_4$ transition state of **3**. These results in combination with the experimentally observed stereoselectivity of the reaction justify our focus on the $^5H_4$ conformers going forward.

In order to address the delocalization observed in our MO calculations and the presence of multiple conformers ($^5H_4$ conformers are expected to react more favorably than $^4H_5$ conformers), we calculated alkene natural bond orbital (NBO) energies for all $^5H_4$ conformers for all glycals within the aforementioned conformational window[69] and obtained a Boltzmann-weighted NBO energy corrected for C_1-C_2 π → C_3-O σ* delocalization (see ESI Table SCY1 – Table SCY14).

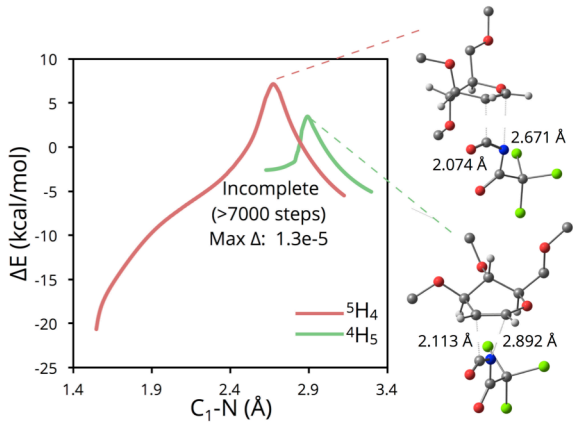

Figure 5. IRC of $^5H_4$ (red) and $^4H_5$ (green) conformers for glycal **3**. Transition state geometry is shown on the right with C_1-N and C_2-C bond distances. Calculations for the $^4H_5$ conformer were halted after 7000 steps with maximum delta of 1.3e-5.

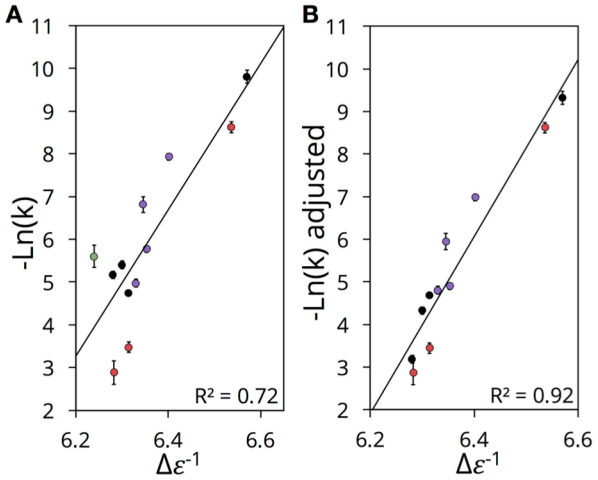

Figure 6. (A) Linear correlation between the logarithm of cycloaddition reaction rate and the corresponding NBO valence energy gap between glycal and trichloroacetyl isocyanate in implicit solvation model. (B) Linear correlation between the logarithm cycloaddition reaction rate adjusted for $^5H_4$ population and the corresponding NBO valence gap between glycal and trichloroacetyl isocyanate with tri-*O*-TES excluded. Red circles – series of 6-*O*-TIPS protected glycals; purple circles – series of 3,4-di-*O*-benzyl protected 6-*O* regioselectively protected glycals; green circle – tri-*O*-TES protected glycal.

The NBO energies are not eigenvalues of the Fock/KS matrix, and as such, the orbital energies are non-physical. These energies correspond to eigenvalues of a hypothetical "Natural Lewis Fock" matrix in which the true Fock matrix in the NBO basis has all off-diagonal elements removed. The energies are thus calculated primarily as a precursor to perturbative analyses of interactions between filled "Lewis-type" and unfilled "Non-Lewis type" NBOs.

The NBO energies do, however, reflect certain important properties of the electronic environment, and these properties are expected to be highly relevant to our present study[61,70]: 1) The natural atomic orbitals (NAOs) from which the NBOs are constructed are sensitive to the partial charge of the parent atom. It can thus be expected that the NAOs from which the glycal alkene NBO is constructed will be slightly more diffuse when electron-donating substituents are present at the 3 and 6 positions, thus destabilizing the NBO energy; 2) The NAOs respond to steric pressure from the neighboring atoms during the orthogonalization process. 3) The π→σ* negative hyperconjugation is re-introduced by including the second-order perturbative delocalization energy between the NBOs.

Compared to the previous single conformer DFT calculations, these new Boltzmann-weighted calculations consider the probability distribution of $^5H_4$ conformers that influence alkene energy. As shown in Figure 6A, the correlation between reaction rate and NBO π energy improves upon that obtained with FMO energies ($R^2 = 0.72$) when conformational sampling was performed. In the case of the tri-*O*-TES protected glycal, we rationalize that the observed deviation from the trend is due to steric constraints arising from the bulk of the protecting group at the C_4 position. Additionally, we modified the experimentally observed reaction rate to account for the percentage of glycal adopting the reactive $^5H_4$ conformation, as determined by our conformational analyses (see ESI methods). With the removal of the tri-*O*-TES protected glycal and adjustment of the experimentally observed reaction rate, the correlation further increases to $R^2 = 0.92$, as shown in Figure 6B.

When comparing the tri-*O*-acetyl (**12**) to the 3,4-di-*O*-acetyl-6-*O*-TIPS protected glycal (**10**), although the *O*-acetyl groups enhance negative hyperconjugation from the allyloxocarbenium system in both cases, there is an activating effect for **10**, as the bulky silyl group locks the glycal in the $^5H_4$ conformation thus inducing an antiperiplanar orientation of the $\sigma_{C3\text{-}O3}$* orbital with the π system. Additionally, while substrates **2** and **13** are comprised of similar $^5H_4/^4H_5$ populations, the increased electron donation from **2** leads to a ~7-fold rate acceleration from 0.0011 s^{-1} to 0.0069 s^{-1} (Table 2). These data support our hypothesis that protecting groups influence glycal reactivity predominantly via π→σ* negative hyperconjugation and interaction with the ring oxygen, accounting for both the observed steric and electronic effects.

As previously observed with the calculated HOMO energies of substrates 1, 3, 4, 12, and 15, an increase in the calculated NBO energy of the alkene of the minimum energy 5H4 conformer is associated with a diminished energy barrier (ΔE‡) for the proposed transition state (Table 4, Figure S21). While this relationship serves as an important tool for validation, it should be noted that NBO calculations are significantly less costly than transition state calculations. Accordingly, an advantage of the NBO method utilized to obtain the correlation identified in Figure 6B is the ability to quickly model the behavior of large populations of the 5H4 conformers of each substrate.

For a small set of glycal cycloadditions involving TCAI, Chmielewski reported that reaction kinetics in chloroform are slower than those in acetonitrile, yet increased when utilizing nitromethane as a solvent.[50] Thus, we conducted cycloaddition reactions for four substrates in chloroform, acetonitrile, or nitromethane to determine the effect of solvent polarity (i.e., dipole moment and dielectric constant) on reaction rate. These three solvents are readily available in deuterated form and while all polar, span a range of dielectric constant (chloroform, acetonitrile, or nitromethane ~5.5, 37.5, and 39.4, respectively) and dipole moment (chloroform, acetonitrile, or nitromethane ~1.01, 3.92, and 3.46 D, respectively). As shown in Figure 7, each of the 4 glycals undergo faster reactions in the more polar acetonitrile and nitromethane solvents compared to chloroform. A slightly slower rate of reaction for **1**, **2**, and **12** occurs in the lower dipole moment solvent of nitromethane in comparison to acetonitrile (3.46 vs 3.92 D). Indeed, the large dipole moment of acetonitrile likely stabilizes the proposed asynchronous transition state and accelerates the observed reaction rate. These findings are in agreement with prior computational studies investigating the effect of solvent on alkene-isocyanate cycloaddition rate.[47]

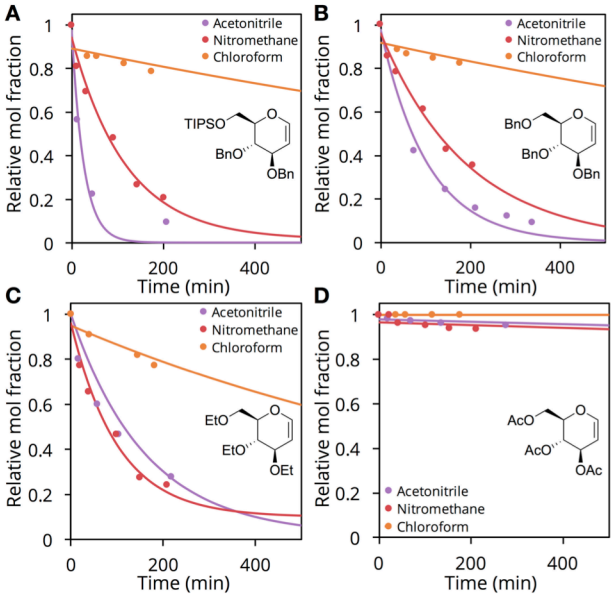

Figure 7. Reaction progress of cycloaddition reactions conducted in deuterated acetonitrile, chloroform, and nitromethane as monitored by ^{1}H-NMR. Starting material mol fraction at each time point was determined by comparing the integration of H1 to the integrations of the [2+2] H1 and [4+2] H1 (determined by $^1H^{13}C$-HSQC). The first-order rate constants were obtained by plotting the logarithm of reaction progress vs time and applying linear regression. The lines of fit shown on each graph were obtained by applying this reaction rate to an exponential decay function. As shown in insets: (A): 3,4-di-O-benzyl-6-O-triisopropylsilyl-D-glucal (**12**); (B): 3,4,6-tri-O-benzyl-D-glucal (**2**); (C): 3,4,6-tri-O-ethyl-D-glucal (**4**); (D): 3,4,6-tri-O-acetyl-D-glucal (**1**).

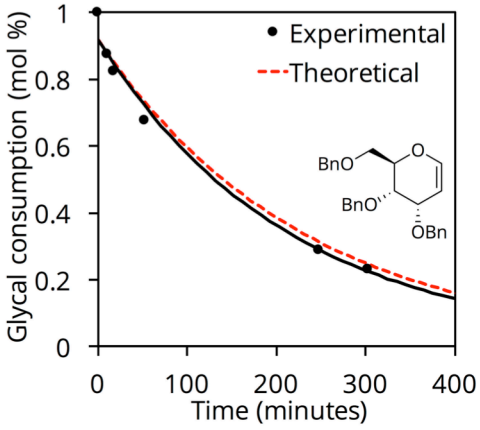

Figure 8. Comparison between experimental and theoretical reaction rate for 3,4,6-tri-*O*-benzyl-D-altral based on NBO calculations adjusted for theoretical $^5H_4$ conformer prevalence; (inset shows structure).

Given that the stereoselectivity of the Staudinger synthesis is determined at least in part by the Hammett constants of the imine and ketene substituents[32], we next investigated the relationship between the experimental cycloaddition [4+2] vs [2+2] reaction selectivity and the theoretical NBO gap. Here, we assume that the stereoelectronic effects governing the [2+2] cycloaddition reaction similarly tune the energetics of the [4+2] cycloaddition, although with differing magnitude. The ratio between [4+2] and [2+2] products remains nearly constant over the course of the reaction; ratios were extracted after 24 h or when the starting material mol fraction was lower than 10%. As shown in Figure S22, similar to the relationship between protecting group bulk and reaction rate, no clear relationship exists between the observed selectivity and theoretical NBO π energy calculation. These data imply that, as expected, glycal reactivity does not bias reaction pathway and that the [2+2] and [4+2] cycloaddition reactions are independent, competing processes.

Importantly, in order to determine if our model can be used to predict the reaction outcome of an unknown compound, we identified and synthesized an additional glycal substrate with potential antibiotic activity[41], which possesses a β-lactam on the β face of the pyranose. This inverted lactam stereoselectivity is achieved via the flipped orientation of the bulky 3'-OH protecting group (*O*-benzyl) in a glycal readily obtained in 2

steps from D-altrose, as we previously described.[65] The $^3J_{H4H5}$ for this glycal is 10.1 Hz indicating a predominance of *pseudo*-equatorially oriented 4'-OH and 6'-OH benzyl groups ($^4H_5$ conformation).[66] Examination of the conformational scans for this glycal, however, indicates a significant population (29%) of $^5H_4$ conformers that facilitates rate prediction according to our previously modeled relationship. Indeed, the calculated NBO energy gap for this substrate is 6.013 eV, corresponding to a rate constant of 0.015 s^{-1}. When accounting for the predominance of reactive $^5H_4$ glycals in the reaction mixture, our calculations predict an experimental rate constant of 0.00435 s^{-1}. The experimentally determined reaction rate of this substrate is 0.00466 s^{-1}, corresponding to a percent error of 1.3% after logarithmic transformation. Figure 8 shows a comparison between the experimental data and computationally predicted data.

CONCLUSIONS

The alkene-isocyanate cycloaddition displays sensitivity to the stereoelectronic effects of protecting groups although, unlike the literature describing this effect in other cycloadditions[71–73], does not involve directly delocalized or conjugated systems. The influence of protecting groups has been studied widely in reference to glycosylation reactions and is in accordance with recent reports that side group orientation plays a significant role in tuning reactivity.[58,60,74,75] In particular, our findings align with those of Bols and coworkers that bulky silyl groups increase the population of ring-flipped conformers with substituents in the axial position ($^5H_4$), thereby modulating reactivity.[74] For example, a single silyl group on the 6'-OH of **11** and **12** increases the predominance of the *pseudo*-axial conformation leading to a significant acceleration in reactivity in parallel with higher calculated alkene energy. Moreover, glycal orientation is only one part of protecting group participation; the electronics of *pseudo*-axially oriented protecting groups play a significant role in further tuning reactivity. For example, glycals **10** and **12** exhibit highly disparate reaction rates despite both possessing a silyl group at the 6'-OH and a predominant $^5H_4$ conformation as the *O*-acetyl group is significantly more electron withdrawing than the *O*-benzyl group. As protecting group effects hold across a variety of glycosylation reactions, our results may be generally applicable to other cycloaddition reactions involving the allyloxycarbenium system, such as the [4+2] cycloaddition of azodicarboxylates to glycals[76] or 1,3-dipolar cycloaddition of alkyl azides to glycals.[77]

Reactivity studies with a library of 17 protected glycal substrates demonstrate that the stereoelectronic influence of protecting groups and solvent stabilization of the reaction intermediate dictate the [2+2] cycloaddition reaction kinetics of glycals and isocyanates. Theoretical glycal HOMO to isocyanate LUMO gaps, calculated on global minimum energy structures, correlate positively and exponentially with the experimentally observed reaction rates in accordance with an Arrhenius model. When restricting glycal HOMO to the alkene contribution using NBOs and accounting for conformational variability from protecting groups oriented *pseudo*-axially (both computationally and experimentally), the correlation significantly improves from R^2=0.72 to R^2=0.92. Transition state calculations reveal that glycal conformation impacts the cycloaddition reaction pathway and support a concerted, asynchronous mechanism with glycals in the $^5H_4$ conformation. In all cases, the glycal C-2 to isocyanate carbon C-C bond forms

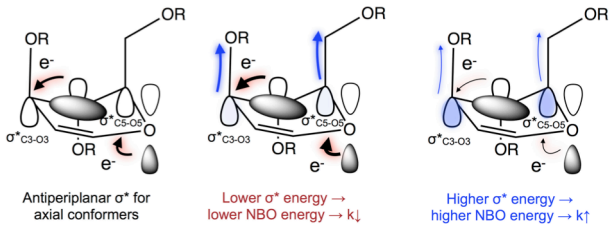

Scheme 3. Negative hyperconjugation explains how protecting groups influence the NBO energy of the glycal alkene to dictate reaction rate. Increased electron density of the alkene improves reaction rate by increasing the enthalpic driving force of the cycloaddition reaction supported by transition state $\Delta H^{\ddagger}$ calculations.

first, followed by ring closure from the isocyanate nitrogen to glycal C-1. The predicted zwitterionic transition state is supported by observations that high dipole solvents, capable of stabilizing charge, increase the reaction rate. Finally, the theoretical model successfully predicts the observed kinetics of a new glycal [2+2] cycloaddition reaction. Together, our results support the hypothesis that negative hyperconjugation from the ring oxygen p-orbitals and the alkene π orbitals to ring $\sigma_{C\text{-}O}$* orbitals significantly impacts glycal reactivity and that careful selection of protecting groups either enhances or diminishes negative hyperconjugation to tune reactivity for predictable β-lactam synthesis (Scheme 3). Specifically, allyloxocarbenium reactivity increases with less electron-withdrawing groups such as the benzyl and p-methoxybenzyl group at all three positions. Highly electron-withdrawing acyl groups and carbonate groups, conversely, strongly deactivate the reactive system. Our findings facilitate the informed synthesis of new β-lactam antibiotics, β-lactamase inhibitors, and β-lactam monomers derived from glycals.

EXPERIMENTAL SECTION

Materials and general methods

D-glucal, tri-*O*-benzyl-D-glucal, tri-*O*-acetyl-D-glucal, and 4,4-dimethoxytrityl chloride were purchased from Carbosynth (San Diego, CA). Tri-*O*-methyl-D-glucal, benzyl bromide, and trimethylamine were purchased from Alfa Aesar (Tewksbury, MA). 4-methoxybenzyl chloride and trichloroacetyl isocyanate were purchased from TCI America (Portland, OR). Deuterated chloroform, acetonitrile, and nitromethane were purchased from Cambridge Isotopes (Tewksbury, MA). All other reagents were purchased from Millipore Sigma (Burlington, MA). All solvents were either purchased anhydrous over molecular sieves or treated using a solvent drying system to remove trace amounts of water. Reactions were monitored by thin-layer chromatography (TLC) analysis, and stained by the solution of potassium permanganate or acidic ceric ammonium molybdate. All ^{1}H-NMR and ^{13}C-NMR spectra were taken with compounds dissolved in $CDCl_3$ [(D, 99.8%) + 0.05% V/V TMS + Silver foil] and the TMS (0 ppm) was used as an internal standard for ^{1}H-NMR spectra. Chemical shifts (δ) are recorded in ppm, coupling constants (J) are reported in Hz. Unless otherwise noted, all reactions were performed under an argon atmosphere using anhydrous solvents and oven-dried glassware and stir bars.

NMR Spectroscopy

Samples were prepared to a concentration of 0.5 M (0.150 mmol) in 300 μL of either $CDCl_3$, CD_3CN, or CD_3NO_2. 2.0 eq of trichloroacetyl isocyanate was added to the solution and the combined solution was quickly mixed and the time noted before adding to a clean, dry NMR tube (Wilmad-LabGlass, Vineland, NJ). The sample was immediately analyzed by ^{1}H-NMR (500 MHz) (Varian, Palo Alto, CA) followed by time points distributed over 24-36 h. After 24 h or after

90% of the starting material had been consumed, we obtained a $^{1}H^{13}C$-HSQC in order to identify and quantify the ratio of the peaks corresponding to H1 of the [2+2] and [4+2] products. All spectral data was processed in MestreNova (Mestrelab Research, Escondido, CA) by first calculating the baseline average by integration of the baseline in 3 different regions without signal. This background average was then subtracted from the integration of each relevant peak (starting material H1, [2+2] H1, [4+2] H1). The subtracted values were added and the percent integration of the starting material of this total value was determined. The ratio of [4+2] to [2+2] products was determined by finding the ratio between integrations of the subtracted integration values after 24 h or after 90% of the starting material had been consumed. To extract rate constants, the logarithm of the reaction progress was plotted against the reaction time and a linear fit equation was obtained ($R^2 > 0.85$ in all cases) whose slope is k, the reaction rate.

Synthetic methods

6-*O*-triisopropylsilyl-D-glucal was prepared as previously described[78]. The crude product was purified by silica column chromatography (4:1 hexanes:ethyl acetate to 1:1 hexanes:ethyl acetate) and the combined fractions were evaporated to dryness to yield 6-*O*-triisopropylsilyl-D-glucal as a viscous, clear oil (yield 79%). Spectroscopic and mass characterization data matched those previously reported.

3,4-di-*O*-benzyl-6-*O*-triisopropylsilyl-D-glucal (**12**) was prepared as previously described[78]. The crude product was purified by silica column chromatography (19:1 hexanes:ethyl acetate to 17:1 hexanes:ethyl acetate) and the combined fractions were evaporated to dryness to yield 3,4-di-*O*-benzyl-6-*O*-triisopropylsilyl-D-glucal as a clear oil (yield 71%). Spectroscopic and mass characterization data matched those previously reported.

3,4-di-*O*-benzyl-D-glucal was prepared as previously described[79]. The crude product was purified by silica column chromatography (4:1 hexanes:ethyl acetate to 2:1 hexanes:ethyl acetate) and the combined fractions were evaporated to dryness to yield 3,4-di-*O*-benzyl-D-glucal as a clear oil that solidified into an amorphous white solid upon storage at -20 ^{o}C (yield 89%). Spectroscopic and mass characterization data matched those previously reported.

3,4,6-tri-*O*-benzyl-D-altral was prepared as previously described[80]. Clear to pale oil. (yield 47% over 5 steps). Spectroscopic and mass characterization data matched those previously reported.

3,4,6-tri-*O*-ethyl-D-glucal (4)

3,4,6-tri-*O*-ethyl-D-glucal was prepared as previously described. D-glucal (400 mg, 2.74 mmol) was dissolved to between 0.2 and 0.3 M in DMF (~10 mL), and cooled to 0 ^{o}C followed by the addition of 3.6 eq of NaH (95% dry, 200 mg, 8.21 mmol). The reaction was allowed to warm to room temperature over 30 minutes followed by cooling to 0 ^{o}C. 3.3 eq of iodoethane (720 µL, 9.04 mmol) was added dropwise and the reaction was allowed to warm to room temperature overnight. The reaction was quenched with methanol, poured into 200 mL of a 0.1 M HCl solution, and extracted 3 times with 50 mL of ether. The combined organic extracts were washed with brine, dried over sodium sulfate, and evaporated to yield the crude product. The crude product was purified by silica column chromatography (10:1 hexanes:ethyl acetate) and fractions were concentrated and evaporated to yield the title compound as a clear oil. (Yield 390 mg, 62%). $[\alpha]_{25}^{D}$ = -0.8 (0.3, CH_3OH). ^{1}H NMR (500 MHz, $CDCl_3$) δ 6.35 (dd, *J* = 6.1, 1.4 Hz, 1H, H1), 4.76 (dd, *J* = 6.1, 2.6 Hz, 1 H, H2), 3.95 (ddd, *J* = 6.4, 2.7, 1.5 Hz, 1H, H3), 3.91 (ddd, *J* = 8.5, 4.9, 3.2 Hz, 1H, H5), 3.81 (m, 1 H), 3.73-3.45 (m, 8H), 1.25-1.16 (m, 9H, Ethyl-C*H*$_3$). $^{13}C\{^{1}H\}$ NMR (126 MHz, $CDCl_3$) δ 144.3 (C1), 100.5 (C2), 76.9 (C5), 76.1 (C3), 74.8 (C4), 69.0-66.9 (*C*H_2CH$_3$), 15.7-15.1 (CH$_2$*C*H$_3$). HRMS ESI+ Q-TOF (*m/z*): $[M+Na]^+$ calcd for $C_{12}H_{22}O_4$: 253.1416; found, 253.1423.

3,4,6-tri-*O*-triethylsilyl-D-glucal (5)

3,4,6-tri-*O*-triethylsilyl-D-glucal was prepared as previously described. D-glucal (400 mg, 2.74 mmol) and 6.6 eq of imidazole (1.23 g, 18.1 mmol) were dissolved to between 0.2 and 0.3 M glycal in DMF (~10 mL), and cooled to 0 ^{o}C. 3.3 eq of chlorotriethylsilane (1.50 mL, 9.04 mmol) was added dropwise and the reaction was allowed to warm to room temperature overnight. The reaction was poured into 200 mL of a 0.1 M HCl solution, and extracted 3 times with 50 mL of ether. The combined organic extracts were washed with brine, dried over sodium sulfate, and evaporated to yield the crude product. The crude product was purified by silica column chromatography (15:1 hexanes:ethyl acetate) and fractions were concentrated and evaporated to yield the title compound as a pale oil. (yield 1.04 g, 78%). $[\alpha]_{25}^{D}$ = -13 (0.3, CH_3OH). ^{1}H NMR (500 MHz, $CDCl_3$) δ 6.32 (d, *J* = 6.2 Hz, 1H, H1), 4.69 (dd, *J* = 6.2, 3.7 Hz, 1 H, H2), 3.91 (d, *J* = 6.7 Hz, 1H, H3), 3.86-3.75 (m, 2H), 1.01-0.87 (m, 27 H, SiCH$_2$C*H*$_3$), 0.70-0.55 (m, 18H, Si*C*H_2CH$_3$). $^{13}C\{^{1}H\}$ NMR (126 MHz, $CDCl_3$) δ 143.2 (C1), 102.0 (C2), 80.0 (C5), 70.5 (C3), 68.2 (C4), 61.6 (C6), 6.9-6.4 (SiCH$_2$*C*H$_3$), 5.2-4.4 (Si*C*H$_2$CH$_3$). HRMS ESI+ Q-TOF (*m/z*): $[M+Na]^+$ calcd for $C_{24}H_{52}O_4Si_3$: 511.3071; found, 511.3136.

3,4,6-tri-*O*-(*p*-methoxybenzyl)-D-glucal (6)

3,4,6-tri-*O*-(*p*-methoxybenzyl)-D-glucal was prepared as previously described. D-glucal (400 mg, 2.74 mmol) was dissolved to between 0.2 and 0.3 M in DMF (~10 mL), and cooled to 0 ^{o}C followed by the addition of 3.6 eq of NaH (95% dry, 200 mg, 8.21 mmol). The reaction was allowed to warm to room temperature over 30 minutes followed by cooling to 0 ^{o}C. 3.3 eq of PMB-Cl (1.2 mL, 9.04 mmol) was added dropwise and the reaction was allowed to warm to room temperature overnight. The reaction was quenched with methanol, poured into 200 mL of a 0.1 M HCl solution, and extracted 3 times with 50 mL of ether. The combined organic extracts were washed with brine, dried over sodium sulfate, and evaporated to yield the crude product. The crude product was purified by silica column chromatography (8:1 hexanes:ethyl acetate) and fractions were concentrated and evaporated to yield the title compound as a clear oil that formed an amorphous white solid upon cooling to -20 ^{o}C. (Yield 1.262 g, 91%). $[\alpha]_{25}^{D}$ = +0.75 (0.25, CH_3OH). ^{1}H NMR (500 MHz, $CDCl_3$) δ 7.30-7.23 (m, 4H, Ar *H*), 7.19-7.12 (m, 2H, Ar *H*), 6.92-6.80 (m, 6H, Ar *H*), 6.41 (dd, *J* = 6.1, 1.3 Hz, 1H, H1), 4.84 (dd, *J* = 6.1, 2.7 Hz, 1H, H2), 4.74 (d, *J* = 10.9 Hz, 1H, C*H*$_2$Ar), 4.60-4.47 (m, 5H, C*H*$_2$Ar), 4.17 (ddd, *J* = 6.3, 2.7, 1.4 Hz, 1H, H3), 4.02 (ddd, *J* = 8.4, 5.1, 2.9 Hz, 1H, H5), 3.84-3.77 (m, 10H, ArOC*H*$_3$ + H4), 3.76-3.69 (m, 2H, C6). $^{13}C\{^{1}H\}$ NMR (126 MHz, $CDCl_3$) δ 159.2 (Ar*C*OCH$_3$), 144.6 (C1), 130.5-129.3 (Ar*C*H), 113.8-113.8 (Ar*C*H), 100.1 (C2), 76.8 (C5), 75.5 (C3), 74.1 (C4), 73.4-70.2 (*C*H$_2$Ar), 68.2 (C6), 55.3 (ArO*C*H$_3$). HRMS ESI+ Q-TOF (*m/z*): $[M+Na]^+$ calcd for $C_{30}H_{34}O_7$: 529.2202; found, 529.2195.

3,4,6-tri-*O*-(2,2,2-trichloroethylcarbonate)-D-glucal (7)

D-glucal (400 mg, 2.74 mmol) was dissolved in 10 mL of pyridine and cooled to 0 ^{o}C. 3.3 eq of 2,2,2-trichloroethyl chloroformate (1.2 mL, 9.04 mmol) was added dropwise and the reaction was allowed to warm to room temperature overnight. The reaction was poured into 200 mL of a 1 M HCl solution and extracted 3 times with 50 mL of ethyl acetate. The combined organic extracts were washed again with 1 M HCl, a saturated solution of $NaHCO_3$, brine, dried over sodium sulfate, and evaporated to yield the crude product. The crude product was purified by silica column chromatography (2:1 hexanes:ethyl acetate) and fractions were concentrated and evaporated to yield the title compound as a clear oil that formed a white amorphous solid upon cooling at -20 ^{o}C. (Yield 1.10 g, 60%). $[\alpha]_{25}^{D}$ = +24 (0.2, CH_3OH). ^{1}H NMR (500 MHz, $CDCl_3$) δ 6.54 (dd, *J* = 6.1, 1.3 Hz, 1H, H1), 5.4 (dddd, *J* = 5.4, 3.2, 1.3, 0.7, 1H, H3), 5.25 (dd, *J* = 7.4, 5.6 Hz, 1H, H4), 5.00 (dd, *J* = 6.2, 3.3 Hz, 1H, H2), 4.85-4.73 (m, 6H, C*H*2CCl3), 4.57 (dd, *J* = 12.7, 6.8 Hz, 1H, H6-1), 4.50-4.41 (m, 2H, H6-2 + H5). $^{13}C\{^{1}H\}$ NMR (126 MHz, $CDCl_3$) δ 153.6-152.9 (*C*O$_3$), 146.4 (C1), 97.6 (C2), 94.1 (*C*Cl$_3$), 77.2-77.0 (*C*H$_2$CCl$_3$), 73.1 (C5),

71.6 (C3), 71.5 (C4), 65.4 (C6). HRMS ESI+ Q-TOF (*m/z*): $[M+Na]^+$ calcd for $C_{15}H_{13}Cl_9O_{10}$: 690.7603; found, 690.7638.

3,4,6-tri-*O*-methoxymethyl-D-glucal (8)

3,4,6-tri-*O*-methoxymethyl-D-glucal was prepared as previously described. D-glucal (400 mg, 2.74 mmol) was dissolved to between 0.2 and 0.3 M in DMF (~10 mL), and cooled to 0 °C followed by the addition of 3.6 eq of NaH (95% dry, 200 mg, 8.21 mmol). The reaction was allowed to warm to room temperature over 30 minutes followed by cooling to 0 °C. 3.3 eq of MOM-Cl (700 µL, 9.04 mmol) was added dropwise and the reaction was allowed to warm to room temperature overnight. The reaction was quenched with methanol, poured into 200 mL of a 0.1 M HCl solution, and extracted 3 times with 50 mL of ether. The combined organic extracts were washed with brine, dried over sodium sulfate, and evaporated to yield the crude product. The crude product was purified by silica column chromatography (3:1 hexanes:ethyl acetate) and fractions were concentrated and evaporated to yield the title compound as a clear oil. (yield 591 mg, 77%). $[\alpha]_{25}^{D}$ = +19 (0.50, CH_3OH). ^{1}H NMR (500 MHz, $CDCl_3$) δ 6.40 (dd, *J* = 6.3, 1.2 Hz, 1H, H1), 4.89-4.84 (m, 1H, H2, OC*H*$_2$O), 4.84-4.78 (m, 1H, OC*H*$_2$O), 4.76-4.72 (m, 1H, OC*H*$_2$O), 4.71-4.64 (m, 3H, OC*H*$_2$O), 4.17 (dddd, *J* = 9.3, 5.9, 3.1, 1.9 Hz, 1H, H5), 4.11 (ddt, *J* = 4.8, 2.3, 1.3 Hz, 1H, H3), 3.88-3.82 (m, 1H, H4), 3.82-3.77 (m, 2H, H6), 3.41-3.35 (m, 9H, OC*H*$_3$). ^{13}C{^{1}H}NMR (126 MHz, $CDCl_3$) δ 144.2 (C1), 100.0 (C2), 96.7-95.4 (O*C*H$_2$O), 76.2 (C5), 73.0 (C4), 71.7 (C3), 65.9 (C6), 56.0-55.5 (O*C*H$_3$). HRMS ESI+ Q-TOF (*m/z*): $[M+Na]^+$ calcd for $C_{12}H_{22}O_7$: 301.1263; found, 301.1257.

Benzyl 3,4-di-*O*-benzyl-D-glucuronal (9)

Benzyl 3,4-di-*O*-benzyl-D-glucuronal was synthesized as previously described. 3,4-di-*O*-benzyl-*D*-glucal (400 mg, 1.22 mmol) and 1.1 eq of diacetoxyiodobenzene (434 mg, 1.35 mmol) were dissolved in 5 mL of DCM and 5 mL of H_2O. The reaction mixture was cooled to 0 °C followed by the addition of 0.2 eq of TEMPO (38.1 mg, 0.24 mmol) and vigorous stirring with monitoring by TLC (permanganate, UV, and bromocresol green). After 4 h, the starting material was found to be consumed and a new spot with a double bond, UV absorbance, pH < 7, and lower R_f (0.1 in 2:1 hexanes:ethyl acetate) appeared. The reaction was poured into 200 mL of 0.1 M HCl and extracted 4 times with 50 mL of ethyl acetate. The combined organic extracts were dried over magnesium sulfate, followed by sodium sulfate, and the solvent was evaporated. The crude residue was then dissolved in 20 mL of DMF, followed by the addition of $KHCO_3$ (3 g, 30 mmol). After stirring at room temperature for 1 h, the solution was cooled to 0 °C and benzyl bromide was added to the solution dropwise (3.42 mL, 28.8 mmol). The reaction was allowed to warm to room temperature overnight and was poured into 250 mL of a 0.1 M HCl solution followed by extraction 4 times with 50 mL of ether. The combined organic extracts were further washed with a saturated $NaHCO_3$ solution, brine, and dried over sodium sulfate. The crude product was purified by silica column chromatography (gradient 10:1 to 6:1 hexanes:ethyl acetate) and fractions were concentrated and evaporated to yield the title compound as a clear oil. (Yield 165 mg, 32% over 2 steps). ^{1}H NMR (500 MHz, $CDCl_3$) δ 7.40-7.17 (m, 15H, Ar*H*), 6.66 (d, *J* = 6.3 Hz, 1H, H1), 5.06 (d, *J* = 12.3 Hz, 1H, ArC*H*$_2$), 5.03 (ddd, *J* = 6.5, 5.0, 1.5 Hz, 1H, H2), 4.88 (d, *J* = 12.3 Hz, 1H, ArC*H*$_2$), 4.83 (dd, *J* = 3.1, 1.3 Hz, 1H, H5), 4.72-4.62 (m, 2H, ArC*H*$_2$), 4.43 (d, *J* = 11.6 Hz, 1H, ArC*H*$_2$), 4.34 (d, *J* = 11.6, 1H, ArC*H*$_2$), 4.22 (td, *J* = 2.9, 1.5 Hz, 1H, H4), 3.86 (ddd, *J* = 4.6, 2.7, 1.2 Hz, 1H, H3). ^{13}C{^{1}H} NMR (126 MHz, $CDCl_3$) δ 168.1 (*C*OOBn), 145.1 (C1), 128.7-127.7 (Ar), 98.6 (C2), 73.3 (C4), 72.8 (C5), 72.0 (Ar*C*H$_2$), 69.4 (Ar*C*H$_2$), 67.7 (C3), 67.0 (Ar*C*H$_2$). ^{1}H and ^{13}C spectroscopy data matched those previously reported[79].

3,4-di-*O*-acetyl-6-*O*-triisopropylsilyl-D-glucal (10)

6-*O*-triisopropylsilyl-D-glucal (400 mg, 1.32 mmol) was dissolved in 10 mL of pyridine and cooled to 0 °C. 5 eq of acetic anhydride (1.25 mL, 13.2 mmol) was added dropwise and the reaction was allowed to warm to room temperature over 3 h while monitoring by TLC. Upon completion, the reaction was poured into 200 mL of a 1 M HCl solution and extracted 3 times with 50 mL of ethyl acetate. The combined organic extracts were washed again with 1 M HCl, a saturated solution of $NaHCO_3$, brine, dried over sodium sulfate, and evaporated to yield the crude product. The crude product was purified by silica column chromatography (3:1 hexanes:ethyl acetate) and fractions were concentrated and evaporated to yield the title compound as a clear oil. (yield 467 mg, 73%). $[\alpha]_{25}^{D}$ = -3 (0.2, CH_3OH). ^{1}H NMR (500 MHz, $CDCl_3$) δ 6.46 (d, *J* = 6.1 Hz, 1H, H1), 5.33-5.26 (m, 2H, H3 + H4), 4.78 (ddd, *J* = 6.2, 2.4, 1.2 Hz, 1H, H2), 4.12 (qt, *J* = 5.1, 2.6 Hz, 1H, H5), 3.89 (d, *J* = 4.8 Hz, 2H), 2.05 (s, 3H, COC*H*$_3$), 2.03 (s, 3H, COC*H*$_3$), 1.05 (m, 21H, Si(*i*-Pr)$_3$). ^{13}C{^{1}H} NMR (126 MHz, $CDCl_3$) δ 170.5 (*C*OCH$_3$), 169.4 (*C*OCH$_3$), 146.0 (C1), 98.1 (C2), 76.8 (C5), 67.6 (C3), 67.3 (C4), 61.4 (C6), 21.1 (CO*C*H$_3$), 20.9 (CO*C*H$_3$), 17.9 (SiCH(*C*H$_3$)$_2$), 11.9 (Si*C*H(CH$_3$)$_2$). HRMS ESI+ Q-TOF (*m/z*): $[M+Na]^+$ calcd for $C_{19}H_{34}O_6Si$: 409.2022; found 409.2024.

3,4-di-*O*-(*p*-methoxybenzyl)-6-*O*-triisopropylsilyl-D-glucal (11)

3,4-di-*O*-(p-methoxybenzyl)-6-*O*-triisopropylsilyl-D-glucal was prepared as previously described. 6-*O*-triisopropylsilyl-D-glucal (400 mg, 1.32 mmol) was dissolved in 10 mL of DMF and cooled to 0 °C followed by the addition of 2.4 eq of NaH (95% dry, 76 mg, 3.17 mmol). The reaction was allowed to warm to room temperature over 30 minutes followed by cooling to 0 °C. 2.2 eq of PMB-Cl (400 µL, 2.90 mmol) was added dropwise and the reaction was allowed to warm to room temperature overnight. The reaction was quenched with methanol, poured into 200 mL of a 0.1 M HCl solution, and extracted 3 times with 50 mL of ether. The combined organic extracts were washed with brine, dried over sodium sulfate, and evaporated to yield the crude product. The crude product was purified by silica column chromatography (5:1 hexanes:ethyl acetate) and fractions were concentrated and evaporated to yield the title compound as a clear to pale oil. (yield 572 mg, 79%). $[\alpha]_{25}^{D}$ = -0.8 (0.3, CH_3OH). ^{1}H NMR (500 MHz, $CDCl_3$) δ 7.28 (ddd, *J* = 9.5, 4.5, 2.6 Hz, 4H, Ar*H*), 6.92 – 6.84 (m, 4H, Ar*H*), 6.39 (dd, *J* = 6.1, 1.4 Hz, 1H, H1), 4.82 (dd, *J* = 6.2, 2.7 Hz, 1H, H2), 4.75 (bq, 2H, ArC*H*$_2$), 4.56 (q, 2H, ArC*H*$_2$), 4.18 (ddt, *J* = 4.3, 2.6, 1.5 Hz, 1H, H3), 4.05 – 3.97 (m, 2H, H6), 3.90 (m, 2H, H4 + H5), 3.81 (s, 6H, ArOC*H*$_3$), 1.22 – 1.01 (m, 21H, Si(*i*-Pr)$_3$). ^{13}C{^{1}H} NMR (126 MHz, $CDCl_3$) δ 159.3 (Ar*C*OCH$_3$), 159.2 (Ar*C*OCH$_3$), 144.7 (C1), 130.7-129.4 (Ar), 113.8-113.8 (Ar), 99.7 (C2), 78.2 (C5), 75.5 (C3), 73.7 (C4), 73.5 (Ar*C*H$_2$), 70.4 (Ar*C*H$_2$), 62.0 (Ar*C*H$_2$), 55.3 (O*C*H$_3$), 18.0 (SiCH$_2$*C*H$_3$), 12.1-12.0 (Si*C*H$_2$CH$_3$). HRMS ESI+ Q-TOF (*m/z*): $[M+Na]^+$ calcd for $C_{31}H_{46}O_6Si$: 565.2961; found 565.2970.

3,4-di-*O*-benzyl-6-*O*-acetyl-D-glucal (13)

3,4-di-*O*-benzyl-6-*O*-acetyl-D-glucal was prepared as previously described. 3,4-di-*O*-benzyl- D-glucal (400 mg, 1.22 mmol) was dissolved in 8 mL of pyridine and cooled to 0 °C. 2 mL of acetic anhydride (21.1 mmol, 17 eq) was added dropwise and the reaction was allowed to warm to room temperature over 3 h while monitoring by TLC. Upon completion, the reaction was poured into 200 mL of a 1 M HCl solution and extracted 3 times with 50 mL of ethyl acetate. The combined organic extracts were washed again with 1 M HCl, a saturated solution of $NaHCO_3$, brine, dried over sodium sulfate, and evaporated to yield the crude product. The crude product was purified by silica column chromatography (4:1 hexanes:ethyl acetate) and fractions were concentrated and evaporated to yield the title compound as a clear oil. (yield 380 mg, 84%). $[\alpha]_{25}^{D}$ = +3 (0.1, CH_3OH). ^{1}H NMR (500 MHz, $CDCl_3$) δ 7.45 – 7.27 (m, 10H, ArH), 6.44 (dd, J = 6.2, 1.3 Hz, 1H, H1), 4.96 (dd, J = 6.2, 2.7 Hz, 1H, H2), 4.90 (d, J = 11.4 Hz, 1H, ArC*H*$_2$), 4.75 – 4.67 (m, 2H, ArC*H*$_2$), 4.60 (d, J = 11.6 Hz, 1H, ArC*H*$_2$), 4.43 (qd, J = 12.1, 4.1 Hz, 2H, H6), 4.27 (ddd, J = 6.0, 2.7, 1.3 Hz, 1H, H3), 4.14 (ddd, J = 8.3, 5.3, 2.7 Hz, 1H, H5), 3.83 (dd, J = 8.6, 6.0 Hz, 1H, H4), 2.08 (s, 3H, COC*H*$_3$). ^{13}C{^{1}H} NMR (126 MHz, $CDCl_3$) δ 170.7 (*C*OCH$_3$), 144.4 (C1), 138.2-137.9 (Ar), 128.7,-127.8 (Ar), 100.1 (C2), 75.5 (C3), 75.1 (C5), 73.9 (C4), 73.9-70.5 (Ar*C*H$_2$), 62.8 (C6), 20.9 (CO*C*H$_3$). HRMS ESI+ Q-TOF (*m/z*): $[M+Na]^+$ calcd for $C_{22}H_{24}O_5$: 391.1521; found 391.1508.

3,4-di-O-benzyl-6-O-methyl-D-glucal (14)

3,4-di-*O*-benzyl- D-glucal (400 mg, 1.22 mmol) was dissolved in 10 mL of DMF and cooled to 0 °C followed by the addition of 1.3 eq of NaH (95% dry, 38 mg, 1.59 mmol). The reaction was allowed to warm to room temperature over 30 minutes followed by cooling to 0 °C. 1.3 eq of methyl iodide (100 µL, 1.61 mmol) was added dropwise and the reaction was allowed to warm to room temperature overnight. The reaction was quenched with methanol, poured into 150 mL of a 0.1 M HCl solution, and extracted 3 times with 30 mL of ether. The combined organic extracts were washed with brine, dried over sodium sulfate, and evaporated to yield the crude product. The crude product was purified by silica column chromatography (6:1 hexanes:ethyl acetate) and fractions were concentrated and evaporated to yield the title compound as a clear to pale oil. (Yield 253 mg, 61%). $[\alpha]_{25}^{D}$ = -7 (0.1, CH_3OH). ^{1}H NMR (500 MHz, $CDCl_3$) δ 7.40 – 7.26 (m, 10H, Ar*H*), 6.42 (dd, J = 6.1, 1.3 Hz, 1H, H1), 4.88 (dd, J = 6.1, 2.7 Hz, 1H, H2), 4.86 (d, J = 11.4 Hz, 1H, ArC*H*$_2$), 4.72 – 4.63 (m, 2H, ArC*H*$_2$), 4.58 (d, J = 11.7 Hz, 1H, ArC*H*$_2$), 4.23 (ddd, J = 6.4, 2.6, 1.4 Hz, 1H, H3), 4.02 (ddd, J = 8.3, 5.2, 2.7 Hz, 1H, H5), 3.83 (dd, J = 8.8, 6.3 Hz, 1H, H4), 3.72 (dd, J = 10.6, 5.2 Hz, 1H, H6-1), 3.67 (dd, J = 10.7, 2.7 Hz, 1H, H6-2), 3.40 (s, 3H, C*H*$_3$). ^{13}C{^{1}H} NMR (126 MHz, $CDCl_3$) δ 144.7 (C1), 138.4-138.2 (Ar), 128.4-127.6 (Ar), 100.1 (C2), 76.7 (C5), 75.8 (C3), 74.4 (C4), 73.8 (Ar*C*H$_2$), 70.9 (C6), 70.4 (Ar*C*H$_2$), 59.2 (*C*H$_3$). HRMS ESI+ Q-TOF (*m/z*): $[M+Na]^+$ calcd for $C_{21}H_{24}O_4$: 363.1572; found 363.1577.

3,4-di-*O*-benzyl-6-*O*-(2,2,2-trichloroethylcarbonate)-D-glucal (15)

3,4-di-*O*-benzyl- D-glucal (400 mg, 1.22 mmol) was dissolved in 10 mL of pyridine and cooled to 0 °C followed by the addition of 1.1 eq of 2,2,2-trichloroethyl chloroformate (190 µL, 1.34 mmol). The reaction was allowed to warm to room temperature overnight. The reaction was quenched with methanol, poured into 150 mL of a 1 M HCl solution, and extracted 3 times with 30 mL of ethyl acetate. The combined organic extracts were washed again with 1 M HCl, a saturated solution of $NaHCO_3$, brine, dried over sodium sulfate, and evaporated to yield the crude product. The crude product was purified by silica column chromatography (2:1 hexanes:ethyl acetate) and fractions were concentrated and evaporated to yield the title compound as a clear oil. (Yield 431 mg, 72%). $[\alpha]_{25}^{D}$ = +5 (0.2, CH_3OH). ^{1}H NMR (500 MHz, $CDCl_3$) δ 7.44 – 7.31 (m, 10H, Ar), 6.44 (dd, *J* = 6.2, 1.3 Hz, 1H, H1), 4.98 (dd, *J* = 6.2, 2.8 Hz, 1H, H2), 4.91 (d, *J* = 11.4 Hz, 1H, ArC*H*$_2$), 4.84 – 4.76 (m, 2H, C*H*$_2$CCl$_3$), 4.75 – 4.68 (m, 2H, ArC*H*$_2$), 4.62 – 4.53 (m, 3H, ArC*H*$_2$ + H6), 4.26 (ddd, J = 6.0, 2.8, 1.3 Hz, 1H, H3), 4.22 (ddd, J = 8.4, 5.6, 2.8 Hz, 1H, H5), 3.86 (dd, J = 8.3, 5.8 Hz, 1H, H4). ^{13}C{^{1}H} NMR (126 MHz, $CDCl_3$) δ 153.9 (*C*O$_3$), 144.3 (C1), 138.1-137.8 (Ar), 128.6-127.7 (Ar), 100.2 (C2), 94.4 (CCl$_3$), 76.9 (*C*H$_2$CCl$_3$), 75.0 (C3), 74.7 (C5), 73.7 (C4), 73.6 (Ar*C*H$_2$), 67.1 (Ar*C*H$_2$). HRMS ESI+ Q-TOF (*m/z*): $[M+Na]^+$ calcd for $C_{23}H_{23}Cl_3O_6$: 523.0458; found 523.0454.

3,4-di-*O*-benzyl-6-*O*-trityl-D-glucal (16)

3,4-di-*O*-benzyl-6-*O*-trityl-D-glucal was prepared as previously described. 3,4-di-*O*-benzyl- D-glucal (400 mg, 1.22 mmol) and 0.1 eq of 4-DMAP (15 mg, 0.12 mmol) was dissolved in 10 mL of pyridine and cooled to 0 °C followed by the addition of 1.2 eq of TrCl (408 mg, 1.46 mmol). The reaction was allowed to warm to room temperature overnight. The reaction was then poured into 150 mL of a 1 M HCl solution, and extracted 3 times with 30 mL of ether. The combined organic extracts were washed again with 1 M HCl, a saturated solution of $NaHCO_3$, brine, dried over sodium sulfate, and evaporated to yield the crude product. The crude product was purified by silica column chromatography (15:1 hexanes:ethyl acetate) and fractions were concentrated and evaporated to yield the title compound as a viscous clear oil. (Yield 254 mg, 36%). $[\alpha]_{25}^{D}$ = +1.3 (0.2, CH_3OH). ^{1}H NMR (500 MHz, $CDCl_3$) δ 7.55 – 7.02 (m, 25H, Ar), 6.54 (dd, J = 6.1, 1.4 Hz, 1H, H1), 4.92 (dd, J = 6.2, 2.6 Hz, 1H, H2), 4.78 (d, J = 11.1 Hz, 1H), 4.67 (d, J = 11.6 Hz, 1H), 4.57 (dd, J = 20.7, 11.3 Hz, 2H), 4.22 (ddt, J = 5.5, 2.5, 1.3 Hz, 1H, H3), 4.10 – 4.00 (m, 2H, H5+H4), 3.59 (dd, J = 10.4, 2.2 Hz, 1H, H6), 3.45 (dd, J = 10.3, 4.0 Hz, 1H, H6). ^{13}C{^{1}H} NMR (126 MHz, $CDCl_3$) δ 144.9 (C1), 143.9 (Ar) , 138.4-138.1 (Ar), 128.8-127.0 (Ar), 99.8 (C2), 86.5 (*C*-Tr), 77.0 (C5), 76.1 (C3), 74.7 (C4), 73.9 (Ar*C*H$_2$), 70.9 (Ar*C*H$_2$), 62.2 (C6). HRMS ESI+ Q-TOF (*m/z*): $[M+Na]^+$ calcd for $C_{39}H_{36}O_4$: 591.2511; found 591.2565.

3,4-di-*O*-benzyl-6-*O*-dimethoxytrityl-D-glucal (17)

3,4-di-*O*-benzyl- D-glucal (400 mg, 1.22 mmol) and 0.1 eq of 4-DMAP (15 mg, 0.12 mmol) was dissolved in 10 mL of pyridine and cooled to 0 °C followed by the addition of 1.2 eq of DMT-Cl (500 mg, 1.46 mmol). The reaction was allowed to warm to room temperature overnight. The reaction was then poured into 150 mL of a 1 M HCl solution, and extracted 3 times with 30 mL of ether. The combined organic extracts were washed again with 1 M HCl, a saturated solution of $NaHCO_3$, brine, dried over sodium sulfate, and evaporated to yield the crude product. The crude product was purified by silica column chromatography (12:1 hexanes:ethyl acetate) and fractions were concentrated and evaporated to yield the title compound as a clear oil. (Yield 404 mg, 53%). $[\alpha]_{25}^{D}$ = +4 (0.1, CH_3OH). ^{1}H NMR (500 MHz, $CDCl_3$) δ 7.58 – 7.51 (m, 2H, Ar*H*), 7.45 – 7.19 (m, 15H, Ar*H*), 7.12 – 7.04 (m, 2H, Ar*H*), 6.88 – 6.79 (m, 4H, Ar*H*), 6.55 (dd, J = 6.1, 1.4 Hz, 1H, H1), 4.93 (dd, J = 6.1, 2.5 Hz, 1H, H2), 4.80 (d, J = 11.0 Hz, 1H, ArC*H*$_2$), 4.69 (d, J = 11.6 Hz, 1H ArC*H*$_2$), 4.59 (dd, J = 25.2, 11.3 Hz, 2H ArC*H*$_2$), 4.24 (ddt, J = 4.1, 2.5, 1.5 Hz, 1H, H3), 4.10 – 4.02 (m, 2H, H5+H4), 3.80 (2s, J = 1.1 Hz, 6H, OC*H*$_3$), 3.60 (dd, J = 10.4, 1.7 Hz, 1H, H6-1), 3.51 – 3.43 (m, 1H, H6-2). ^{13}C{^{1}H} NMR (126 MHz, $CDCl_3$) δ 158.5 (Ar*C*OCH$_3$), 145.0 (C1), 138.4-138.2 (Ar), 136.2-136.0 (Ar), 130.2-126.7 (Ar), 113.1 (*o*-Ar(OCH$_3$)), 99.9 (C2), 85.9 (*C*-DMT), 77.1 (C5), 76.3 (C3), 74.7 (C4), 73.9 (Ar*C*H$_2$), 70.9 (Ar*C*H$_2$), 61.9 (C6), 55.2 (ArO*C*H$_3$). HRMS ESI+ Q-TOF (*m/z*): $[M+Na]^+$ calcd for $C_{41}H_{40}O_6$: 651.2723; found 651.2713.

ASSOCIATED CONTENT

Supporting Information

The Supporting Information is available free of charge on the ACS Publications website at DOI:

Supplemental figures, general experimental methods, synthetic methods, spectra, and computational output (PDF) are available (158 pages)

AUTHOR INFORMATION

Corresponding Author

* mgrin@bu.edu

ORCID

Mark W. Grinstaff: 0000-0002-5453-3668

Anant S. Balijepalli: 0000-0003-4686-8123

Aladin Hamoud: 0000-0001-9928-2096

James H. McNeely:

Author Contributions

† - these authors contributed equally to this work. ASB synthesized all compounds, performed all cycloaddition experiments, performed all experimental data workup, and wrote the manuscript. JHM performed all DFT and NBO calculations, transition state calculations, and helped write and edit the manuscript. AH helped synthesize compounds for characterization. MWG provided mentorship, writing, and editing of the manuscript.

ACKNOWLEDGMENT

This work was supported in part by BU and DOD USU (HU0001810012). NMR facilities at Boston University are sup-

ported by the NSF (CHE-0619339). The authors would like to acknowledge Daniel Burke for help in the synthesis of **6**, **9**, and **14** for characterization and Dr. Norman C. Lee for help in obtaining HRMS spectra.

REFERENCES

(1) Kong, K.-F.; Schneper, L.; Mathee, K. Beta-Lactam Antibiotics: From Antibiosis to Resistance and Bacteriology. *APMIS* **2010**, *118* (1), 1–36. https://doi.org/10.1111/j.1600-0463.2009.02563.x.

(2) Dürckheimer, W.; Blumbach, J.; Lattrell, R.; Scheunemann, K. H. Recent Developments in the Field of β-Lactam Antibiotics. *Angew. Chemie Int. Ed. English* **1985**, *24* (3), 180–202. https://doi.org/10.1002/anie.198501801.

(3) Andersson, I.; Terwisscha van Scheltinga, A. C.; Valegård, K. Towards New β-Lactam Antibiotics. *Cell. Mol. Life Sci.* **2001**, *58* (12), 1897–1906. https://doi.org/10.1007/PL00000825.

(4) Bush, K.; MacIelag, M. J. New β-Lactam Antibiotics and β-Lactamase Inhibitors. *Expert Opin. Ther. Pat.* **2010**, *20* (10), 1277–1293. https://doi.org/10.1517/13543776.2010.515588.

(5) Graf, R.; Lohaus, G.; Börner, K.; Schmidt, E.; Bestian, H. β-Lactams, Their Polymerization and Use as Raw Materials for Fibers. *Angew. Chemie Int. Ed. English* **1962**, *1* (9), 481–488. https://doi.org/10.1002/anie.196204811.

(6) Fernandes, R.; Amador, P.; Prudêncio, C. β-Lactams: Chemical Structure, Mode of Action, and Mechanisms of Resistance. *Rev. Med. Microbiol.* **2013**, *24* (1), 7–17. https://doi.org/10.1097/MRM.0b013e3283587727.

(7) Thompson, R. L. Cephalosporin, Carbapenem, and Monobactam Antibiotics. *Mayo Clin. Proc.* **1987**, *62* (9), 821–834.

(8) Hellinger, W. C.; Brewer, N. S. Carbapenems and Monobactams: Imipenem, Meropenem, and Aztreonam. *Mayo Clin. Proc.* **1999**, *74* (4), 420–434. https://doi.org/10.4065/74.4.420.

(9) Nagata, W.; Narisada, M.; Yoshioka, M.; Yoshida, T.; Onoue, H. [Studies on Oxacephems, an Artificial Type of Beta-Lactam Antibiotics]. *Yakugaku Zasshi* **1991**, *111* (2), 77–102.

(10) Wright, A. J.; Wilkowske, C. J. The Penicillins. *Mayo Clin. Proc.* **1991**, *66* (10), 1047–1063.

(11) Onishi, H. R.; Daoust, D. R.; Zimmerman, S. B.; Hendlin, D.; Stapley, E. O. Cefoxitin, a Semisynthetic Cephamycin Antibiotic: Resistance to Beta-Lactamase Inactivation. *Antimicrob. Agents Chemother.* **1974**, *5* (1), 38–48. https://doi.org/10.1128/aac.5.1.38.

(12) Fu, K. P.; Neu, H. C. Antibacterial Activity of Ceftizoxime, a Beta-Lactamase-Stable Cephalosporin. *Antimicrob. Agents Chemother.* **1980**, *17* (4), 583–590. https://doi.org/10.1128/aac.17.4.583.

(13) Saudagar, P. S.; Survase, S. A.; Singhal, R. S. Clavulanic Acid: A Review. *Biotechnol. Adv.* **2008**, *26* (4), 335–351. https://doi.org/10.1016/J.BIOTECHADV.2008.03.002.

(14) Finlay, J.; Miller, L.; Poupard, J. A. A Review of the Antimicrobial Activity of Clavulanate. *J. Antimicrob. Chemother.* **2003**, *52* (1), 18–23. https://doi.org/10.1093/jac/dkg286.

(15) Cierpucha, M.; Panfil, I.; Danh, T. T.; Chmielewski, M.; Kurzatkowski, W.; Rajnisz, A.; Solecka, J. Synthesis of 3-Substituted-Clavams: Antifungal Properties, DD-Peptidase and β-Lactamase Inhibition. *J. Antibiot. (Tokyo).* **2007**, *60* (10), 622–632. https://doi.org/10.1038/ja.2007.80.

(16) Deopura, B. L.; Alagirusamy, R.; Joshi, M.; Gupta, B. Polyesters and Polyamides. *Polyesters Polyam.* **2008**, 1–608. https://doi.org/10.1533/9781845694609.

(17) Zhang, J.; Kissounko, D. A.; Lee, S. E.; Gellman, S. H.; Stahl, S. S. Access to Poly-β-Peptides with Functionalized Side Chains and End Groups via Controlled Ring-Opening Polymerization of β-Lactams. *J. Am. Chem. Soc.* **2009**, *131* (4), 1589–1597. https://doi.org/10.1021/ja8069192.

(18) Zhang, J.; Gellman, S. H.; Stahl, S. S. Kinetics of Anionic Ring-Opening Polymerization of Variously Substituted β-Lactams: Homopolymerization and Copolymerization. *Macromolecules* **2010**, *43* (13), 5618–5626. https://doi.org/10.1021/ma1010809.

(19) Emilie A. Porter; Bernard Weisblum; Samuel H. Gellman. Mimicry of Host-Defense Peptides by Unnatural Oligomers: Antimicrobial β-Peptides. *J. Am. Chem. Soc.* **2002**, *124* (25), 7324–7330. https://doi.org/10.1021/JA0260871.

(20) Mowery, B. P.; Lee, S. E.; Kissounko, D. A.; Epand, R. F.; Epand, R. M.; Weisblum, B.; Stahl, S. S.; Gellman, S. H. Mimicry of Antimicrobial Host-Defense Peptides by Random Copolymers. *J. Am. Chem. Soc.* **2007**, *129* (50), 15474–15476. https://doi.org/10.1021/ja077288d.

(21) Mowery, B. P.; Lindner, A. H.; Weisblum, B.; Stahl, S. S.; Gellman, S. H. Structure−activity Relationships among Random Nylon-3 Copolymers That Mimic Antibacterial Host-Defense Peptides. *J. Am. Chem. Soc.* **2009**, *131* (28), 9735–9745. https://doi.org/10.1021/ja901613g.

(22) Liu, R.; Chen, X.; Hayouka, Z.; Chakraborty, S.; Falk, S. P.; Weisblum, B.; Masters, K. S.; Gellman, S. H. Nylon-3 Polymers with Selective Antifungal Activity. *J. Am. Chem. Soc.* **2013**, *135* (14), 5270–5273. https://doi.org/10.1021/ja4006404.

(23) Karlsson, A. J.; Flessner, R. M.; Gellman, S. H.; Lynn, D. M.; Palecek, S. P. Polyelectrolyte Multilayers Fabricated from Antifungal β-Peptides: Design of Surfaces That Exhibit Antifungal Activity Against Candida Albicans. *Biomacromolecules* **2010**, *11* (9), 2321–2328. https://doi.org/10.1021/bm100424s.

(24) Nadithe, V.; Liu, R.; Killinger, B. A.; Movassaghian, S.; Kim, N. H.; Moszczynska, A. B.; Masters, K. S.; Gellman, S. H.; Merkel, O. M. Screening Nylon-3 Polymers, a New Class of Cationic Amphiphiles, for SiRNA Delivery. *Mol. Pharm.* **2015**, *12* (2), 362–374. https://doi.org/10.1021/mp5004724.

(25) Dane, E. L.; Grinstaff, M. W. Poly-Amido-Saccharides: Synthesis via Anionic Polymerization of a β-Lactam Sugar Monomer. *J. Am. Chem. Soc.* **2012**, *134* (39), 16255–16264. https://doi.org/10.1021/ja305900r.

(26) Dane, E. L.; Chin, S. L.; Grinstaff, M. W. Synthetic Enantiopure Carbohydrate Polymers That Are Highly Soluble in Water and Noncytotoxic. *ACS Macro Lett.* **2013**, *2* (10), 887–890. https://doi.org/10.1021/mz400394r.

(27) Stidham, S. E.; Chin, S. L.; Dane, E. L.; Grinstaff, M. W. Carboxylated Glucuronic Poly-Amido-Saccharides as Protein Stabilizing Agents. *J. Am. Chem. Soc.* **2014**, *136* (27), 9544–9547. https://doi.org/10.1021/ja5036804.

(28) Dane, E. L.; Ballok, A. E.; O'Toole, G. A.; Grinstaff, M. W. Synthesis of Bioinspired Carbohydrate Amphiphiles That Promote and Inhibit Biofilms. *Chem. Sci.* **2014**, *5* (2). https://doi.org/10.1039/C3SC52777H.

(29) Xiao, R.; Zeng, J.; Grinstaff, M. W. Biologically Active Branched Polysaccharide Mimetics: Synthesis via Ring-Opening Polymerization of a Maltose-Based β-Lactam. *ACS Macro Lett.* **2018**, *7* (7), 772–777. https://doi.org/10.1021/acsmacrolett.8b00302.

(30) Hosseyni, S.; Jarrahpour, A. Recent Advances in β-Lactam Synthesis. *Org. Biomol. Chem.* **2018**, *16* (38), 6840–6852. https://doi.org/10.1039/C8OB01833B.

(31) Palomo, C.; Aizpurua, J.; Ganboa, I.; Oiarbide, M. Asymmetric Synthesis of β-Lactams Through the Staudinger Reaction and Their Use as Building Blocks of Natural and Nonnatural Products. *Curr. Med. Chem.* **2004**, *11* (14), 1837–1872. https://doi.org/10.2174/0929867043364900.

(32) Jiao, L.; Liang, Y.; Xu, J. Origin of the Relative Stereoselectivity of the β-Lactam Formation in the Staudinger Reaction. *J. Am. Chem. Soc.* **2006**, *128* (18), 6060–6069. https://doi.org/10.1021/ja056711k.

(33) Cossío, F. P.; Arrieta, A.; Sierra, M. A. The Mechanism of the Ketene−Imine (Staudinger) Reaction in Its Centennial: Still an Unsolved Problem? *Acc. Chem. Res.* **2008**, *41* (8), 925–936. https://doi.org/10.1021/ar800033j.

(34) Podlech, J.; Linder, M. R. Cycloadditions of Ketenes Generated in the Wolff Rearrangement. Stereoselective Synthesis of Aminoalkyl-Substituted β-Lactams from α-Amino Acids. *J. Org. Chem.* **1997**, *62* (17), 5873–5883. https://doi.org/10.1021/jo9705069.

(35) Huang, L.; Zhao, W.; Staples, R. J.; Wulff, W. D. Multifaceted Interception of 2-Chloro-2-Oxoacetic Anhydrides: A Catalytic Asymmetric Synthesis of β-Lactams. *Chem. Sci.* **2013**, *4* (2), 622–628. https://doi.org/10.1039/C2SC21240D.

(36) Fontana, F.; Tron, G. C.; Barbero, N.; Ferrini, S.; Thomas, S. P.; Aggarwal, V. K. Stereoselective Synthesis of Trans-β-Lactams

by Palladium-Catalysed Carbonylation of Vinyl Aziridines. *Chem. Commun.* **2010**, *46* (2), 267–269. https://doi.org/10.1039/B920564K.

(37) Michalak, M.; Stodulski, M.; Stecko, S.; Mames, A.; Panfil, I.; Soluch, M.; Furman, B.; Chmielewski, M. A Formal Synthesis of Ezetimibe via Cycloaddition/Rearrangement Cascade Reaction. *J. Org. Chem.* **2011**, *76* (16), 6931–6936. https://doi.org/10.1021/jo2010846.

(38) Stecko, S.; Furman, B.; Chmielewski, M. Kinugasa Reaction: An "ugly Duckling" of b-Lactam Chemistry. *Tetrahedron* **2014**, *70*, 7817–7844. https://doi.org/10.1016/j.tet.2014.06.024.

(39) Taguchi, Y.; Tsuchiya, T.; Oishi, A.; Shibuya, I. Synthesis of β-Lactams from Isocyanates and Vinyl Ethers under High Pressure. *Bull. Chem. Soc. Jpn.* **1996**, *69* (6), 1667–1672. https://doi.org/10.1246/bcsj.69.1667.

(40) Barrett, A. G.; Betts, M. J.; Fenwick, A. Acyl and Sulfonyl Isocyanates in β-Lactam Synthesis. *J. Org. Chem.* **1985**, *50* (2), 169–175. https://doi.org/10.1021/jo00202a006.

(41) Chmielewski, M.; Kałuza, Z.; Furman, B. Stereocontrolled Synthesis of 1-Oxabicyclic β-Lactam Antibiotics via [2 + 2]Cycloaddition of Isocyanates to Sugar Vinyl Ethers. *Chem. Commun.* **1996**, No. 24, 2689–2696. https://doi.org/10.1039/CC9960002689.

(42) Kałza, Z.; Furman, B.; Chmielewski, M. Asymmetric Induction in [2+2]Cycloaddition of Chlorosulfonyl Isocyanate to 1,2-O-Isopropylidene-5-O-Vinyl-d-Glycofuranoses. *Tetrahedron: Asymmetry* **1995**, *6* (7), 1719–1730. https://doi.org/10.1016/0957-4166(95)00218-E.

(43) Furman, B.; Borsuk, K.; Kaluza, Z.; Lysek, R.; Chmielewski, M. Stereochemistry of [2+2]Cycloaddition of Chlorosulfonyl Isocyanate to Olefins. *Curr. Org. Chem.* **2004**, *8* (6), 463–473. https://doi.org/10.2174/1385272043485792.

(44) Cossío, F. P.; Lecea, B.; Lopez, X.; Roa, G.; Arrieta, A.; Ugalde, J. M. An Ab Initio Study on the Mechanism of the Alkene–Isocyanate Cycloaddition Reaction to Form β-Lactams. *J. Chem. Soc., Chem. Commun.* **1993**, No. 18, 1450–1452. https://doi.org/10.1039/C39930001450.

(45) Williams, C. .; Whitehead, M. . Semi-Empirical Study of Isocyanate Geometries, and β-Lactam Formation through Alkene-Isocyanate Cyclo-Addition Reactions. *J. Mol. Struct. THEOCHEM* **1999**, *491* (1–3), 93–101. https://doi.org/10.1016/S0166-1280(99)00092-5.

(46) Arrieta, A.; Lecea, B.; Cossío, F. P. Computational Studies on the Synthesis of β-Lactams via [2+2] Thermal Cycloadditions. **2010**, 313–347. https://doi.org/10.1007/7081_2009_10.

(47) Cossio, F. P.; Roa, G.; Lecea, B.; Ugalde, J. M. Substituent and Solvent Effects in the [2 + 2] Cycloaddition Reaction between Olefins and Isocyanates. *J. Am. Chem. Soc.* **1995**, *117* (49), 12306–12313. https://doi.org/10.1021/ja00154a033.

(48) Kałuza, Z.; Abramski, W.; Bełzecki, C.; Grodner, J.; Mostowicz, D.; Urbański, R.; Chmielewski, M. Cycloaddition of Chlorosulfonyl Isocyanate to Sugar Vinyl Ethers. *Synlett* **1994**, *1994* (7), 539–541. https://doi.org/10.1055/s-1994-22921.

(49) Kałuza, Z.; Fudong, W.; Bełzecki, C.; Chmielewski, M. Synthesis of β-Lactams from Sugar Vinyl Ethers and Isocyanates. *Tetrahedron Lett.* **1989**, *30* (38), 5171–5172. https://doi.org/10.1016/S0040-4039(01)93477-X.

(50) Kaluza, Z.; Chmielewski, M. Synthesis of 1-Oxabicyclic β-Lactam Precursors from 4,6-O-Benzylidene-D-Allal. *Tetrahedron* **1989**, *45* (22), 7195–7200. https://doi.org/10.1016/S0040-4020(01)89183-3.

(51) Chmielewski, M.; Kaluza, Z.; Salański, P.; Jurczak, J. High-Pressure [2 + 2]Cyloaddition of Acyl Isocyanates to Glycals. *High Press. Res.* **1993**, *11* (1–3), 171–176. https://doi.org/10.1080/08957959208201704.

(52) Bełżecki, C.; Urbański, R.; Urbańczyk-Lipkowska, Z.; Chmielewski, M. Synthesis of 1-Oxacephems from D-Arabinal and L-Rhamnal. *Tetrahedron* **1997**, *53* (41), 14153–14168. https://doi.org/10.1016/S0040-4020(97)00917-4.

(53) Mootoo, D. R.; Konradsson, P.; Udodong, U.; Fraser-Reid, B. Armed and Disarmed N-Pentenyl Glycosides in Saccharide Couplings Leading to Oligosaccharides. *J. Am. Chem. Soc.* **1988**, *110* (16), 5583–5584. https://doi.org/10.1021/ja00224a060.

(54) Fraser-Reid, B.; Wu, Z.; Udodong, U. E.; Ottosson, H. Armed/Disarmed Effects in Glycosyl Donors: Rationalization and Sidetracking. *J. Org. Chem.* **1990**, *55* (25), 6068–6070. https://doi.org/10.1021/jo00312a004.

(55) Fraser-Reid, B.; López, J. C. Armed-Disarmed Effects in Carbohydrate Chemistry: History, Synthetic and Mechanistic Studies. *Top. Curr. Chem.* **2011**, *301*, 1–29. https://doi.org/10.1007/128_2010_105.

(56) Glaudemans, C. P. J.; Fletcher, H. G. Long-Range Effects of Acyl Groups in the Solvolysis of Glycofuranosyl Halides. The Synthesis of 2,3-Di-O-Benzyl-5-O-p-Nitrobenzoyl-α-D-Arabinofuranosyl Chloride and of 2-O-Benzyl-3,5-Di-O-p-Nitrobenzoyl-α-D-Arabinofuranosyl Chloride. *J. Am. Chem. Soc.* **1965**, *87* (20), 4636–4641. https://doi.org/10.1021/ja00948a041.

(57) Friesen, R. W.; Danishefsky, S. J. Controlled Oxidative Coupling of Glycals: A New Strategy for the Rapid Assembly of Oligosaccharides. *J. Am. Chem. Soc.* **1989**, *111*, 6656–6660. https://doi.org/10.1002/chin.198949283.

(58) Pederson, C.; Nordstrøm, L. U.; Bols, M. "Super Armed" Glycosyl Donors: Conformational Arming of Thioglycosides by Silylation. *J. Am. Chem. Soc.* **2007**, *129* (29), 9222–9235.

(59) Bandara, M. D.; Yasomanee, J. P.; Rath, N. P.; Pedersen, C. M.; Bols, M.; Demchenko, A. V. Conformationally Superarmed S-Ethyl Glycosyl Donors as Effective Building Blocks for Chemoselective Oligosaccharide Synthesis in One Pot. *Org. Biomol. Chem.* **2017**, *15* (3), 559–563. https://doi.org/10.1039/c6ob02498j.

(60) Crich, D.; Li, M. Revisiting the Armed-Disarmed Concept: The Importance of Anomeric Configuration in the Activation of S-Benzoxazolyl Glycosides. *Org. Lett.* **2007**, *9* (21), 4115–4118. https://doi.org/10.1021/ol701466u.

(61) Domingo, L. R.; Chamorro, E.; Pérez, P. Understanding the Reactivity of Captodative Ethylenes in Polar Cycloaddition Reactions. A Theoretical Study. *J. Org. Chem.* **2008**, *73* (12), 4615–4624. https://doi.org/10.1021/jo800572a.

(62) Domingo, L. R. Molecular Electron Density Theory: A Modern View of Reactivity in Organic Chemistry. *Molecules* **2016**, *21* (10), 1319.

(63) Shellhamer, D. F.; Bunting, S. A.; Hickle, K. R.; Horn, P. C.; Milligan, J. C.; Shipowick, D. E.; Smith, L. B.; Vandenbroek, D. J.; Perry, M. C.; Boatz, J. A. Kinetic Studies on the Reaction of Chlorosulfonyl Isocyanate with Monofluoroalkenes: Experimental Evidence for Both Stepwise and Concerted Mechanisms and a Pre-Equilibrium Complex on the Reaction Pathway. *J. Org. Chem.* **2013**, *78* (2), 246–252. https://doi.org/10.1021/jo3016488.

(64) Henrik Helligsø Jensen; Lars Ulrik Nordstrøm; Bols, M. The Disarming Effect of the 4,6-Acetal Group on Glycoside Reactivity: Torsional or Electronic? *J. Am. Chem. Soc.* **2004**, *126* (30), 9205–9213. https://doi.org/10.1021/JA047578J.

(65) Crich, D.; Li, L. 4,6-O-Benzylidene-Directed β-Mannopyranosylation and α-Glucopyranosylation: The 2-Deoxy-2-Fluoro- and 3-Deoxy-3-Fluoro- Series of Donors and the Importance of the O2-C2-C3-O3 Interaction. *J. Org. Chem.* **2007**, *72* (5), 1681. https://doi.org/10.1021/JO062294Y.

(66) Chalmers, A. A.; Hall, R. H. Conformational Studies of D-Glycals by 1H Nuclear Magnetic Resonance Spectroscopy. *J. Chem. Soc. Perkin Trans. 2* **1974**, No. 6, 728–732. https://doi.org/10.1039/P29740000728.

(67) Ussing, B. R.; Hang, C.; Singleton, D. A. Dynamic Effects on the Periselectivity, Rate, Isotope Effects, and Mechanism of Cycloadditions of Ketenes with Cyclopentadiene. *J. Am. Chem. Soc.* **2006**, *128* (23), 7594–7607. https://doi.org/10.1021/ja0606024.

(68) Gonzalez-James, O. M.; Kwan, E. E.; Singleton, D. A. Entropic Intermediates and Hidden Rate-Limiting Steps in Seemingly Concerted Cycloadditions. Observation, Prediction, and Origin of an Isotope Effect on Recrossing. *J. Am. Chem. Soc.* **2012**, *134* (4), 1914–1917. https://doi.org/10.1021/ja208779k.

(69) Weinhold, F. Natural Bond Orbital Analysis: A Critical Overview of Relationships to Alternative Bonding Perspectives. *J. Comput. Chem.* **2012**, *33* (30), 2363–2379. https://doi.org/10.1002/jcc.23060.

(70) Lee, M.; Zimmermann-Steffens, S. G.; Arey, J. S.; Fenner, K.; Von Gunten, U. Development of Prediction Models for the

Reactivity of Organic Compounds with Ozone in Aqueous Solution by Quantum Chemical Calculations: The Role of Delocalized and Localized Molecular Orbitals. *Environ. Sci. Technol.* **2015**, *49* (16), 9925–9935. https://doi.org/10.1021/acs.est.5b00902.

(71) Domingo, L. R.; Aurell, M. J.; Pérez, P.; Contreras, R. Quantitative Characterization of the Global Electrophilicity Power of Common Diene/Dienophile Pairs in Diels–Alder Reactions. *Tetrahedron* **2002**, *58* (22), 4417–4423. https://doi.org/10.1016/S0040-4020(02)00410-6.

(72) Boger, D. L.; Curran, T. T. Diels-Alder Reactions of 1-Aza-1,3-Butadienes: Room Temperature, Endo-Selective LUMOdiene-Controlled [4 + 2] Cycloaddition Reactions of N-Sulfonyl-4-(Ethoxycarbonyl)-1-Aza-1,3-Butadienes. *J. Org. Chem.* **1990**, *55* (20), 5439–5442. https://doi.org/10.1021/jo00307a009.

(73) Pérez, P.; Domingo, L. R.; Aurell, M. J.; Contreras, R. Quantitative Characterization of the Global Electrophilicity Pattern of Some Reagents Involved in 1,3-Dipolar Cycloaddition Reactions. *Tetrahedron* **2003**, *59* (17), 3117–3125. https://doi.org/10.1016/S0040-4020(03)00374-0.

(74) Bols, M.; Pedersen, C. M. Silyl-Protective Groups Influencing the Reactivity and Selectivity in Glycosylations. *Beilstein J. Org. Chem.* **2017**, *13* (1), 93–105. https://doi.org/10.3762/bjoc.13.12.

(75) Bandara, M. D.; Yasomanee, J. P.; Rath, N. P.; Pedersen, C. M.; Bols, M.; Demchenko, A. V. Conformationally Superarmed S-Ethyl Glycosyl Donors as Effective Building Blocks for Chemoselective Oligosaccharide Synthesis in One Pot. *Org. Biomol. Chem.* **2017**, *15* (3), 559–563. https://doi.org/10.1039/c6ob02498j.

(76) Fitzsimmons, B.; Leblanc, Y.; Rokach, J. [4+2] Cycloaddition of Azodicarboxylate and Glycals: A Novel and Simple Method for the Preparation of 2-Amino-2-Deoxy Carbohydrates. *J. Am. Chem. Soc.* **1987**, *109*, 285–286.

(77) Dahl, R. S.; Finney, N. S. A Surprising Dipolar Cycloaddition Provides Ready Access to Aminoglycosides. *J. Am. Chem. Soc.* **2004**, *126*, 8356–8357. https://doi.org/10.1021/ja0319238.

(78) Lellouche, J. P.; Koeller, S. The Particular Sensitivity of Silyl Ethers of D-Glucal toward Two Vilsmeier - Haack Reagents POCl 3 ·DMF and (CF 3 SO 2) 2 O·DMF. Their Unique and Selective Conversion to the Corresponding C(6)-O-Formates. *J. Org. Chem.* **2001**, *66* (3), 693–696. https://doi.org/10.1021/jo005540t.

(79) Mikula, H.; Matscheko, D.; Schwarz, M.; Hametner, C.; Fröhlich, J. Improved and Large-Scale Synthesis of Different Protected d-Glucuronals. *Carbohydr. Res.* **2013**, *370*, 19–23. https://doi.org/10.1016/J.CARRES.2013.01.007.

(80) Xiao, R.; Dane, E. L.; Zeng, J.; McKnight, C. J.; Grinstaff, M. W. Synthesis of Altrose Poly-Amido-Saccharides with β-N-(1→2)-D-Amide Linkages: A Right-Handed Helical Conformation Engineered in at the Monomer Level. *J. Am. Chem. Soc.* **2017**, jacs.7b07405. https://doi.org/10.1021/jacs.7b07405.